IX. DESCRIPTION, TYPES AND DISTRIBUTION OF MANGANESE NODULES IN THE GH78-1 AREA

Tomoyuki Moritani, Makoto Yuasa, Tsunekazu Ajiki and Eiji Kuboki**

Introduction

In the GH78-1 area manganese nodules were obtained from 37 stations among 39 total ones. Here we report the preliminary results of the observation done mainly on-board the ship. Types of manganese nodule are first described following the classification established in the previous cruise (MORITANI *et al.* 1977), and then the pattern of nodule distribution is discussed in relation to the topography, substrate stratigraphy and surface sediment types. In addition, a short description on the obtained and observed rocks from several stations are included in this chapter.

Method of nodule study

Bottom sampling was done at stations over a distance of usually 1° or about 110 km apart, and in some area at those additionally placed in the middle of usual grids, or spaced more closely in case of the detailed survey. For regular sampling, three types of sampler were used: Okean (Ocean)–70 grab which can take a bottom portion of about 0.5 m^2 square area and 0.35 m depth, double-spade box corer with a catch area of 0.16 m^2 and 0.4 m depth, and the freefall photograb with a catch area of about 0.116 m^2. The freefall photograb sampler was dropped usually in two sets at each sampling site by the wire-lined samplers of Okean–70 grab or double-spade box corer, in a very close distance each other from a few hundred to a few thousand meters.

Nodule samples obtained were described and studied on board for 1) observation of occurrence and morphology in and outside samplers, type classification, size classification, measurement of weight and calculation of abundance (kg/m^2); 2) photographing whole nodules on plates with respective catch square areas of each sampler, and typical samples on plate with 5 cm grid scale; and 3) observation of internal structures of the nodules on cut section. Determination of mineral composition by X-ray diffractometer and chemical analysis were carried out in the onshore laboratory after the cruise as described in Chapter XV (FAKIOGLU *et al.*, in this report) and in Chapter XIV (NAKAO *et al.*, in this report).

The results are summarized in the sample lists (Table IX-2) and photograph log (Fig. IX-3). The relation of manganese nodules to the geological environments was examined by referring to other data of related studies, such as topography, sedimentology, and acoustic survey.

Occurrence of manganese nodules

Similarly in the previous GH76-1 and GH77-1 areas, it was confirmed that

* Metal Mining Agency of Japan, Tokyo

Table IX-1 Morphological classification of manganese nodules (After MORITANI *et al.*, 1977)

Types	Size	Shape	Surface texture
Sr	small-medium	spheroidal/ellipsoidal	rough (granular or micro-botryoidal)
SPr	small-medium	spheroidal/ellipsoidal/intergrown	rough
SEr	medium-large	spheroidal/ellipsoidal	rough-botryoidal
Db	medium-large	discoidal/ellipsoidal	rough-botryoidal
Ss/SPs	small-medium	spheroidal/intergrown	smooth (smooth or micro-granular)
DPs	small-medium	flattened/elongated/discoidal/ intergrown	smooth
ISs	large	irregular/spheroidal/flattened/ angular/fractured	smooth
IDPs	large	irregular/flattened/discoidal/ fractured	smooth
V	small-large	variable depending on the nucleus forms (Shark's teeth, nodule fragments etc.)	smooth or rough

Each type name is represented by the symbols taken from the initial of each morphological term. Here, each size class roughly corresponds in maximum diameter; small- < 4 cm, medium-4-6 cm, large- > 6 cm. Morphological symbols indicate; S-spheroidal, E-ellipsoidal, D-discoidal, P-poly or intergrown, I-irregular, V-variable, F-faceted, B-biological, T-tabular or flattened.

within the sediment column of 35 cm to 40 cm deep almost in all cases manganese nodules of the GH78-1 area occurred on the sea bottom surface or exactly speaking in the water-sediment interface though their state was more or less different as more exposed or buried. However, exceptionally at St. 1057–2 a clear horizon of buried manganese nodules was recognized at a depth of 25 cm below the bottom surface.

Types of manganese nodules

The morphological types were determined according to the classification schema established in the previous GH76-1 cruise as shown in Table IX-1. This is based both on the surface structure, smooth(s) and rough(r) or botryoidal(b) and on the shapes, such as spheroidal(S), ellipsoidal(E), discoidal(D), intergrown or polylobate(P), irregular(I) and variable(V) forms, and each type is represented by the combination of the initials of both terms as Sr or Ss. Nine types such as Sr, SPr, SEr, Db, Ss/SPs, DPs, ISs, IDPs and Vs were originally recognized in the GH76-1 area, and these were applicable as a whole for the GH77-1 area without modification though there were some slight variations. As theoretically thought, there are expected variations or gradations of such nodule types both in surface structure and shape. In the GH78-1 area, the intermediate type of surface structure, smooth to rough(s·r), was newly distinguished, and for shape type original Ss/SPs was separated as Ss and SPs. Altogether, as shown in Table IX-2, 17 types were identified in this area. They are for rough surface type group Sr, SPr, SEr, Db and Vr, for intermediate type group Ss·r, SPs·r, Ds·r and IDPs·r, and for smooth type group Ss, SPs, Ds, DPs, ISs, IDs, IDPs and Vs. Variation in shapes relates to the inner structures or nucleus shape of manganese nodules. As nuclei there were recognized sedimentary rocks,

Table IX-2. List of sampled and observed

Station No.	Sample No.	Position						Depth (m)	Morphological type
		Latitude			Longitude				
1036	G(B)604	08	00	3 N	176	57	1 E	5,251	ISs, Ss
	FG73-1	08	00	1 N	176	57	0 E	5,174	SPs
	FG73-2	08	00	1 N	176	56	7 E	5,184	ISs. Ss
1036A	D261	08	00	9 N	176	57	1 E	5,174	ISs, SPs, Ss, DPs
		△08	01	0 N	176	55	7 E	5,329	
1037	FG74-1	09	03	1 N	176	58	6 E	5,020	ISs, Ss, Vs
	FG74-2	09	03	3 N	176	58	5 E	5,040	ISs, Ss, Vs
1037-1	G(B)605-1	08	59	9 N	176	58	2 E	5,225	SPs, Ss
1038	FG75-1	09	59	5 N	176	58	1 E	5.952	ISs, Vs
	FG75-2	09	59	5 N	176	58	0 E	5,952	ISs, SPs, Ss, Vs
1038-A	G640	10	00	2 N	176	59	3 E	6,140	Vs, DPs, IDPs, SPs, Ss
	FG113-1	09	59	8 N	176	59	5 E	6,140	ISs, SPs, Vs
	FG113-2	09	59	9 N	176	59	6 E	6,160	ISs, SPs, IDPs, Vs
1039	FG76-1	10	00	3 N	177	00	3 E	5,020	DPs, Vs
1039-A	G641	11	00	4 N	176	59	6 E	5,242	IDPs
	FG114-1	11	00	5 N	176	59	5 E	5,225	SPs, IDs, DPs
	FG114-2	11	00	5 N	176	59	6 E	5,215	IDs
1040	G(B)608	11	57	5 N	176	57	4 E	5,381	IDPs, DPs
1041	G(B)609	12	58	9 N	177	00	1 E	5.690	SPs, Ss
	FG78-1	12	59	2 N	177	00	3 E	5,680	Ss, Vs
	FG78-2	12	59	4 N	177	00	3 E	5,680	Ss, Vs
1042	G(B)610	12	59	9 N	177	58	4 E	5,803	SPr, Sr
	FG79-1	13	00	0 N	177	58	3 E	5,813	SPr
	FG79-2	13	00	0 N	177	58	5 E	5,813	Sr, Db
1043	G611	12	00	9 N	178	00	0 E	5,608	Sr, Vr
	FG80-1	12	00	9 N	177	59	4 E	5.608	Sr, Vr
	FG80-2	12	00	9 N	177	59	6 E	5,618	Sr, SPr, Dr, Vr
1044	FG81-1	11	00	5 N	178	00	7 E	5,360	SPs, Ss
	FG81-2	11	00	5 N	178	00	8 E	5.370	SPs, Ss
1044-1	G612-1	11	00	3 N	178	00	6 E	5,322	Ss·r, SPs·r
1045	G613	09	59	3 N	178	00	6 E	5,380	DPs, SPs, Ss
	FG82-1	09	59	5 N	178	00	6 E	5,246	DPs
1046	G614	09	01	3 N	177	59	8 E	5,474	Ss·r, SPs·r
	FG83-1	09	01	4 N	178	00	2 E	5,463	Ss·r, SPs·r
	FG83-2	09	01	5 N	178	00	4 E	5,433	Ss·r, SPs·r
1047	G615	07	59	2 N	178	01	7 E	5,660	Sr, SPr
	FG84-1	07	59	1 N	178	00	9 E	5,660	Sr, SPr
	FG84-2	07	59	1 N	178	01	0 E	5,649	Sr, SPr
1048	G(B)616	07	59	2 N	179	00	2 E	5.183	SPs, DPs
	FG85-1	07	59	7 N	179	00	0 E	5,153	SPs
	FG85-2	07	59	7 N	179	00	2 E	5,153	SPs
1048-1	G616-1	07	59	6 N	179	00	2 E	5,143	ISs, IDPs, DPs, Ss
1049	G617	09	04	4 N	179	02	4 E	5.983	Sr, SPr
	FG86-1	09	04	5 N	179	01	4 E	5,983	Sr, SPr
	FG86-2	09	04	5 N	179	01	6 E	5,973	Sr
1050	G618	09	59	7 N	179	00	7 E	5,603	SPs, DPs
	FG87-1	09	59	3 N	178	59	9 E	5,618	DPs
	FG87-2	09	59	3 N	179	00	1 E	5,618	DPs

manganesc nodules of GH87-1 cruise

Total weignt (kg)	Abundance	(kg/m²)	Number of size fraction(cm) >10	10-8	8-6	6-4	4-2	2-1	<1	Thickness of outermost crust (mm) and nucleus material.
5.2	●	32.5			9	29	16			(5). shark's tooth
3.7	●	32.0	1	2	8	24	1			(5)
3.5	●	30.3			6	24	21			(5)
200										
2.4	●	20.8			8	12	15			(3-5)
3.0	●	26.0			2	25	48	5		(3)
1.7	⊙	10.6			2	28	38			(3) shark's tooth
1.5	⊙	13.0				16	57	8		
0.8	◬	6.9				8	26			
8.2	⊙	16.7		1	4	113	282	2		(1-2)
2.1	⊙	18.2				11	116	1		
2.4	●	20.7				15	98			
0.25	△	2.2			1	2				
6.6	⊙	13.5			5	78	488	23		(<1)
1.75	⊙	15.1			2	18	95	13		(2)
0.01	+	0.09					2			
1.2	◬	7.5			1	17	86	35		Organic matter, clay
<0.1	+							4	2	
<0.1	+							2	7	
<0.1	+							2	11	
<0.1	+						2	3		
<0.1	+						1	1		
<0.1	+						3	7		
0.9	△	1.8	1				10	23	7	
0.1	◇	0.9			1	3	31	26	11	
0.1	◇	0.9		1	1	3	12	7	6	
0.34	△	2.9				2	15	26	2	
0.24	△	2.1				1	13	14	2	
1.9	△	3.9				12	125	224	84	(2-3), shark's tooth
9.9	●	20.2			4	92	578	85	M	(1-2), rock fragment, clay
<0.1	+	0.09				1				
1.1	△	(2.2)				3	100	305	258	
0.7	◬	6.0					99	157	38	
0.9	◬	7.7				1	121	167	45	
1.4	△	2.9				4	99	467	236	
0.3	△	2.6				1	24	133	40	
0.5	△	4.3			1	2	29	99	69	
1.3	◬	8.1		1	4	2	8			
<0.1	+							1		
0.8	◬	6.9			3	8	9	3		(7-12)
12.5	●	25.5	2	8	32	61	314	701		(6-18) (2), clay derived from volcanics
1.7	△	(3.5)				8	86	197	39	(9-12), shark's tooth
1.1	◬	9.5				6	54	91	20	
1.1	◬	9.5				5	50	105	21	
3.05	◬	6.2		1	1	38	307	362	92	(3-5), rock fragment
1.4	⊙	12.1			1	8	129	85	8	
<0.1	+						2	2		

Table IX-2. List of sampled and observed

Station No.	Sample No.	Position						Depth (m)	Morphological tpye
		Latitude			Longitude				
1051	G619	10	59	1 N	179	01	1 E	5,235	DPs, IDPs, Vs
	F G88-1	10	59	5 N	179	01	1 E	5,245	DPs, Vs
	F G88-2	10	59	6 N	179	01	2 E	5,245	Vs
1052	G620	12	00	3 N	179	01	5 E	5,926	Sr, SPr
	F G89-1	12	00	1 N	179	01	7 E	5,931	Sr, SPr
	F G89-2	12	00	1 N	179	01	8 E	5,931	Sr, SPr
1053	G621	12	57	5 N	179	01	3 E	4,910	Ss, DPs
	F G90-1	12	58	8 N	179	00	6 E	4,782	Ss, SPs, DPs
	F G90-2	12	58	8 N	179	00	8 E	4,813	Ss, SPs, DPs
1054	G622	12	59	6 N	179	59	8 E	5,053	Ss, SPs, Vs
	F G91-2	12	59	8 N	179	59	8 E	4,762	SPs, Ss
1055	G(B)625	12	01	1 N	179	58	7 E	5,962	Sr, SPr
	F G94-1	12	00	0 N	179	59	3 E	5,952	Sr, SPr
	F G94-2	12	00	0 N	179	59	3 E	5,952	Sr, SPr
1056	G(B)626	10	58	8 N	179	58	6 W	5,930	Ss·r, SPs·r, DPs·r
	F G95-1	10	58	5 N	179	59	0 W	5,952	Ss·r,SPs·r,DPs·r,IDPs·r
	F G95-2	10	58	5 N	179	58	9 W	5,930	SPs·r, IDPs·r, IDPs·r
1057	F G96-1	09	59	9 N	180	00	0	5,942	Ss, SPs, DPs
	F G96-2	09	59	9 N	180	00	0	5,952	Ss, SPs
1057-2	G627-2-A	09	59	4 N	180	00	0	5,952	DPs, ISs, Ss, SPs
	G627-2-B	09	59	4 N	180	00	0	5,952	IDPs, DPs, Ss, SPs
1059	G629	07	59	6 N	179	59	4 W	6,056	Sr, SPr, SEr
	F G98-1	07	59	3 N	179	59	9 W	6,056	
	F G98-2	07	59	3 N	179	59	8 W	6,056	Sr, SPr, SEr
1060	G(B)623	12	59	1 N	178	59	5 W	5,720	Ss, SPs, DPs
	F G92-1	12	59	4 N	179	00	1 W	5,700	DPs
	F G92-2	12	59	5 N	179	00	1 W	5,710	DPs
1061	G(B)624	11	59	8 N	179	02	6 W	5,632	Ss·r,SPs·r,IDPs·r,Ds·r
	F G93-1	11	59	9 N	179	03	0 W	5,639	Ss, SPs, IDPs
	F G93-2	11	59	9 N	179	02	9 W	5,634	Ss, SPs, DPs
1064	F G100-1	07	33	2 N	179	30	0 E	5,245	Vs, SPs, DPs
	F G100-2	07	33	2 N	179	30	1 E	5,328	Ss, SPs, Vs, IDPs
1065	G632	08	32	2 N	179	28	4 E	6,159	SEr, SPr, Dr
	F G101-1	08	31	6 N	179	28	7 E	6,159	Sr
	F G101-2	08	31	7 N	179	28	7 E	6,159	SEr, SPr, Dr
1066	F G102-1	08	30	7 N	178	31	0 E	6,263	SPs, Vs
	F G102-2	08	30	7 N	178	31	2 E	6,263	SPs, Vs
1067	G634	07	29	1 N	178	31	3 E	5,250	SPs, Ss, ISs, Vs, Ds
	F G103-1	07	29	4 N	178	30	7 E	5,370	SPs, Vs
	F G103-2	07	29	5 N	178	30	8 E	5,340	SPs, Ss, ISs
1068	F G104-1	07	29	6 N	177	30	4 E	5,433	SPs
	F G104-2	07	29	6 N	177	30	6 E	5,423	SPs
1069	F G105-1	08	30	4 N	177	29	5 E	5,464	SPs, Ss
	F G105-2	08	30	5 N	177	29	7 E	5,433	Ss, SPs, ISs, Vs
1070	G636	07	33	8 N	176	33	0 E	4,947	Ss, SPs
	F G106-1	07	33	4 N	176	33	3 E	4,968	Ss, SPs
	F G106-2	07	33	6 N	176	33	4 E	4,948	Ss, SPs, Vs, IDPs
1071	G637	08	30	5 N	176	30	4 E	5,020	SPs, ISs, Vs

manganese nodules of GH78-1 cruise

Total weight (kg)	Abundance	(kg/m²)	Number of size fraction (cm) >10	10-8	8-6	6-4	4-2	2-1	<1	Thickness of outermost crust (mm) and nucleus material.
7.3	⊙	14.9	3	6	19	47	166	307	M	(1-10), clay
1.6	⊙	13.8			1	4	86	132	52	
0.1	◇	0.9				1	2	1	1	
1.5	△	3.1		1	1	18	19	10		(3-4), shark's tooth
0.1	◇	0.9				2	2	4	1	
<0.1	+						1	1		
0.9	△	(1.8)				2	72	212		
0.3	△	2.6				1	3	69	24	
<0.1	+							3	2	
11.7	●	23.9			1	93	950	538	M	
0.6	◬	5.2		1		3	21	1	4	
0.1	◇	0.6				2	3	8	1	
0.1	◇	0.9				1	1	12	1	
<0.1	+	0.09					2	7	2	
1.5	◬	9.4			1	29	53	3		(1-5)
1.3	⊙	11.2				8	161	83	2	
2.0	⊙	17.3			1	10	135	28	5	(1-2), rock fragment
1.2	⊙	10.4		2	1	8	15	4		(0.5-1), rock
2.2	⊙	19.0			1	23	21	1	M	(7-20), shark's tooth
7.5	⊙	15.3	1	7	13	77	188	81		(2-7), (5) surface type
2.5	◬	5.1		2	4	26	89	53		(1>)(-2) buried type
0.9	△	1.8		1		1	59	35		
	×									rock fragment
0.1	◇	0.9					9	14	16	
1.2	◬	7.5				1	119	268		
0.25	△	2.2				1	14	2	2	
0.5	△	4.3				3	16	7	M	
0.5	△	3.1				4	2	5	2	
0.7	◬	6.1				3	32	20	2	
0.5	△	4.3				1	32	17		
0.2	△	1.7	1				1			
3.9	●	33.7	1	5	3	6	45	42		(3)
0.15	△	1.3				2	2	2		
<0.1	+							1		
<0.1	+						1	4		
2.0	⊙	17.3				18	98	32	1	
1.8	⊙	15.5				2	186	286		
9.1	⊙	18.6		3	18	46	72	1		(4-5), clay derived from volcanics
3.3	●	28.5			3	25	28			
3.9	●	33.7			11	26	3			(3-5),clay, shark's tooth
2.05	⊙	17.7		1	6	17	106	15		
3.8	●	32.9			8	36	4			
4.4	●	38.1			1	34	11			(3-6), volcanic clay
3.1	●	26.8			1	33	19	1		(4-5), clay
24.1	●	49.2			20	176	157	21	1	
1.9	⊙	16.4			1	16	22	15		
0.6	◬	(5.2)				5	8			
15.2	●	31.0			15	127	179	3		

Table IX-2. List of sampled and observed

Station No.	Sample No.	Position						Depth (m)	Morphological type
		Latitude			Longitude				
1071	FG107-2	08	29	5 N	176	30	3 E	4,989	Vs, ISs
1072	D262	▽08	30	1 N	176	59	4 E	5,723	Ss, SPs, ISs, Vs
		△08	29	8 N	176	57	8 E	5,536	
	FG108-1	08	29	8 N	177	00	8 E	5,754	SPs, Vs, ISs
	FG108-2	08	29	8 N	177	01	0 E	5,774	SPs, ISs, Vs
1073	FG109-1	09	30	0 N	177	00	0 E	5,164	SPs, ISs, Vs
	FG109-2	09	28	0 N	177	00	0 E	5,287	SPs, Vs
	FG109-4	09	24	2 N	176	59	8 E	5,464	ISs, SPs, Vs, IDPs
	FG109-5	09	25	2 N	177	01	8 E	5,350	Vs, ISs, SPs
	FG109-6	09	27	2 N	177	01	7 E	5,329	SPs, Vs
	FG109-7	09	29	3 N	177	01	7 E	5,183	SPs, ISs, Vs
	FG109-8	09	31	4 N	177	01	7 E	5,123	SPs, ISs, Vs
1074	FG110-1	09	30	7 N	176	30	5 E	5,235	SPs, Vs
	FG110-2	09	30	7 N	176	30	3 E	5,225	SPs, ISs
1076	FG112-1	09	28	6 N	177	30	1 E	5,454	Sr, SPr
	FG112-2	09	28	6 N	177	30	2 E	5,464	Sr, SPr, Vr

The abundance in the parentheses shows the probably incorrect values due to the grab sampler. M: Many small fragments including broken ones.

volcanic rocks, clayey materials, shark's teeth, fragments of broken nodule etc. Shape types are not likely to have close relation to nodule mineralogy and chemistry. On the contrary, the surface structure types are important regarding nodule mineralogy and chemistry. The surface structure relates to nodule occurrence in the water-sediment interface as smooth(s) type in more exposed state and rough(r) type in more buried state. This seems to show the condition of nodule growth as precipitation of metal components from sea water in exposed state and precipitation from interstitial water in buried state respectively, reflecting on the difference in mineralogy and chemistry of nodules as discussed in Chapters XIV and XV in this report.

Generally speaking, the nodule types of the GH78-1 area have similarity to those of the GH77-1 and then of GH76-1 areas. But a characteristic trend can be pointed out in that larger size nodules of Ss or SPs types are more predominant in the GH78-1 area, though this trend was already seen in the GH77-1 area, as compared with smaller size nodules of Ss/SPs type in GH76-1 area. Particularly, larger size Ss type with remarkable sphericity like cannon ball shape is recognized in some stations of the south-western mountainous part of the GH78-1 aera, such as Sts. 1036, 1037, 1067 and 1070.

Also, it is interesting that the above mentioned buried nodules of St. 1057–2 are of s type group similar to that on the surface, suggesting possibility of burial after their growth on the bottom surface and then stop of growth after burial.

Distribution of manganese nodules

Two generalized maps were made to show the trend of the regional distribution of manganese nodules and its relations to the geological environment.

manganese nodules of GH78-1 cruise

Total weight (kg)	Abundance	(kg/m²)	Number of size fraction (cm) >10	10-8	8-6	6-4	4-2	2-1	<1	Thickness of outermost crust (mm) and nucleus material.
2.4	●	20.7				2	14	1		
80										
4.4	●	38.1			8	20	37	4		
4.0	●	34.6			11	10	26	2		(3-5)
3.1	●	26.8				3	20	37		(2-4)
1.4	◉	12.1				2	119	208		
3.7	●	32.0	1	2	4	13	101	30		
3.8	●	32.8			1	40	68			(1-5)
1.7	◉	14.7				18	180	132		(1-2) clay, organics
3.1	●	26.8			2	29	65	2		(2-3)
2.2	◉	19.0			3	27	45			(2-3)
3.0	●	25.9			2	16	116	13		
2.8	●	24.2		1		43	44	3		
0.0[4]	◇	0.35						13	13	
0.3[4]	△	2.9					25	49	30	

imperfect sampling, judged from the sea bottom photograph data by freefall photo-

+<0.1, ◇ 0.1-1.0 △ 1.0-5.0, ▲ 5.0-10, ◉ 10-20, ● >20 kg/m²

Fig. IX-1 shows the distribution of both abundance and types of all nodules, together with that of surface sediment types. Fig. IX-2 represents a simplified distribution of nodule abundance in way of isopleth (iso-abundance line).

The local variation in nodule types and abundance in a limited station area is generally small, judging from the data by Okean-70 grab or double spade box corer, and simultaneously used two freefall photograb samplers. About nodule abundance though some larger difference in value are shown at several stations, such as Sts. 1039, 1045, 1048. 1050, 1051, 1053, 1057 and 1064, all the smallest grade values are thought due to mechanically imperfect catch of the bottom probably caused by the existence of large rock fragment or rock bed, and also to obtained rock samples themselves in stead of manganese nodules. Thus as far as nodule abundance is concerned, the grade values are similar in one station area, being within nearest two grades. However, as for type variation there are only two cases in which both s type and s·r type exist together in one station area at Sts. 1044 and 1061. As already mentioned, the vertical distribution of manganese nodules in the sediment column of 35 cm and 40 cm depth was confirmed in the obtained samples by Okean-70 grab and double-spade box corer respectively. Almost in all cases nodules were found on the bottom sediment surface, or in the water-sediment interface. One exception is St. 1057-2 where a horison of buried nodules occurred at the depth of 25 cm below the bottom surface. But, the buried nodules were s type similar to those on the sediment surface.

As shown in regional distribution map of manganese nodule abundance (Fig. IX-2), marked area of highest grade value above 20.0 kg/m² is in the south-west mountainous area and some local ones are in the northeastern seamount

area and in two parts of central to southeastern deep sea basin. Also, broad zone of higher grade values of 10–20 kg/m^2 extends with branches along the latitudes around 10°N and 11°N of the central part of the deep sea basin, while the lower grade value areas lie, one in the northwestern abyssal plain and the others in the southeastern deep sea basin to the southward from around the latitude 10°N.

This regional distribution features of nodule abundance shows good harmony with regional topography. The highest grade abundance areas seem to be confined to the mountainous or ragged topography with thinner acoustic trasparent layer of Type A (Unit I) particularly in the southwestern mountainous area, and the higher grade abundance areas to the repeated hills and troughs area of the central deep sea basin with rather thin acoustic transparent layer of Type A (Unit I). The zonal area of the above mentioned higher grade abundance represents the westward extension of the highest grade abundance zone in the adjacent GH77-1 area. Similarly, the lower grade abundance area in the southeastern deep sea basin to the southward from around the latitude 10°N corresponds to the northwestward extension of general topographic depression to the northwest of Magellan Rise in the adjacent GH77-1 area. Here the thick acoustic turbidites layer of Type C (Unit I) presumably derived from the Magellan Rise, buries the depression.

The other lower grade abundance area remarkably coinsides with the flat topography of the northeastern abyssal plain. In this case, however, the acoustic layer of Type A (Unit I) is rather thinner.

As shown in Fig. IX-1, the types of surface sediment show roughly zonal distribution. From calcareous ooze or calcareous-siliceous ooze at topographic highs in the southwestern mountainous area, towards northeast broad zone of siliceous clay and then wider zone of deep sea clay in the central and southeastern deep sea basin are developed. And there are distributed locally a zeolitic mud zone in the deep sea clay zone in the northwestern abyssal plain, a siliceous ooze zone between siliceous clay and deep sea clay zones in the southeastern deep sea basin. On this zonal distribution it is difficult to point out clear relations between surface sediment types and nodule types or abundance, except that calcareous ooze and siliceous ooze zones coincide to part of none or scarce nodule abundance as generally recognized in the GH77-1 or GH76-1 areas. However, the highest grade abundance value of 49.2 kg/m^2 was found on calcareous-siliceous ooze at St. 1070, though we have not enough data to interprete this unusual association.

The nodule types, especially of r and s surface structure type groups rather show close relation with distribution of the nodule abundance. The distribution of r type nodules is more or less restricted to the lower grade abundance area less than 10.0 kg/m^2 in the southeastern deep sea basins to southward from around latitude 10°N, and in the northern area including the northwestern abyssal plain.

In conclusion, both the nodule abundance and, to some extent, types especially on surface structure seem to have relation to the sedimentation rate as the total effects of topographic condition, and bottom current regime, resulting abundant nodule distribution in lower sedimentation rate areas.

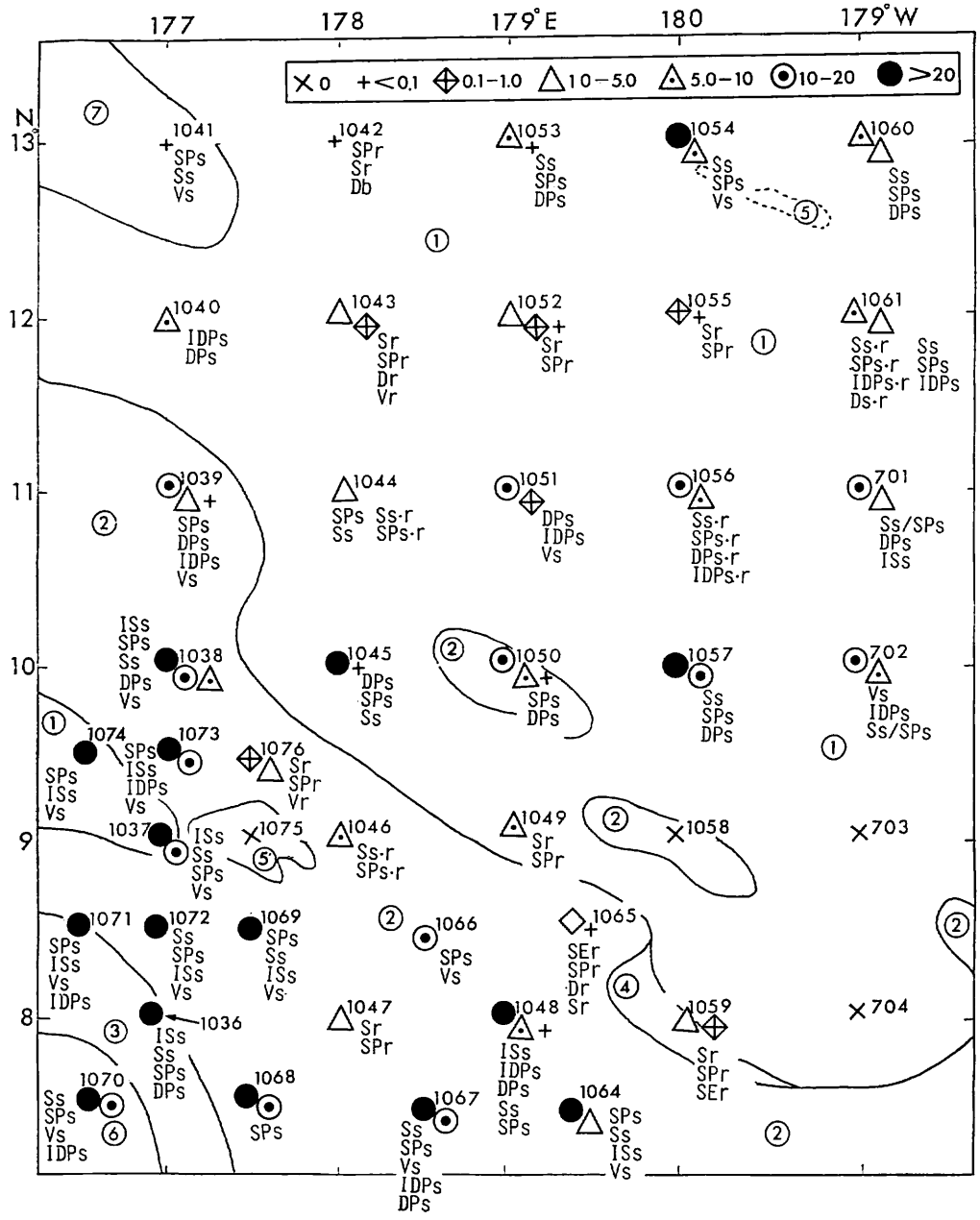

Fig. IX-1 Generalized map of distribution of surface sediments, manganese nodule types and abundance. Abundance is shown in kg/m^2, and two or three different marks of it in one station indicate variation of its values according to the different sampling points within the same station area. Surface sediment data, after NAKAO and SUZUKI (Chapt. VII, in this report), are shown by the circle numbers: 1. Deep sea clay, 2. Siliceous clay, 3. Calcareous-siliceous clay, 4. Siliceous ooze, 5. Calcareous ooze, 6. Calcareous-siliceous ooze, 7. Zeolitic mud.

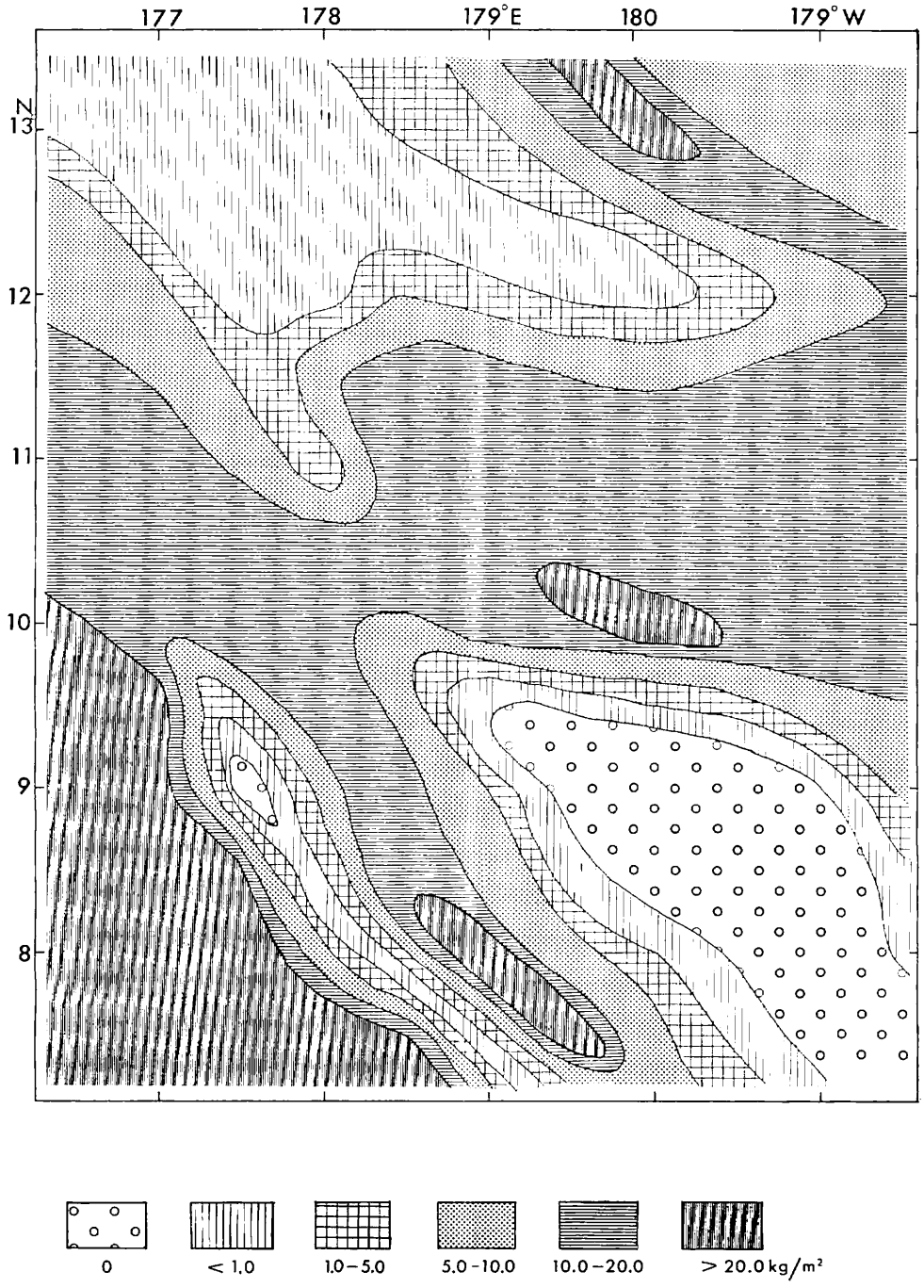

Fig. IX-2 Distribution of manganese nodule abundance (in kg/m^2). The lines show isopachs of Unit I. This map shows only the general trend basing on the data from roughly spaced sampling stations.

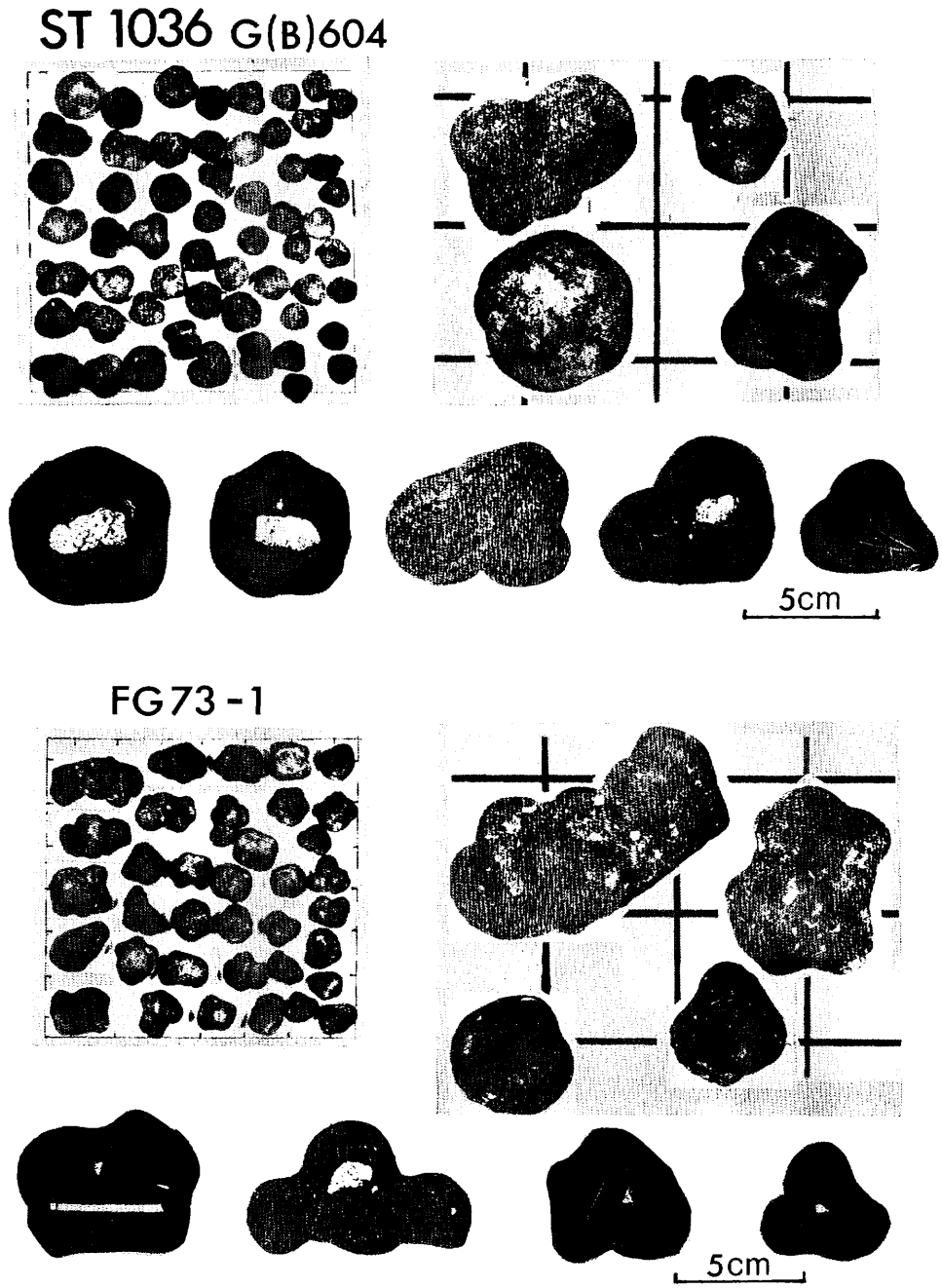

(1)

Fig. IX-3 (1-44) Photograph log of manganese nodule from each station. Whole samples caught by each samples were photographed on square plates with respective catch areas, as 34 cm×34 cm=0.116 m^2 for freefall grab(FG), 40 cm×40 cm=0.16 m^2 for spade box corer (G(B)), and 70 cm×70 cm=0.49 m^2 for Okean-70 type grab(G). Typical samples were photographed on the 5 cm grid scale. Cross sections of same typical samples are shown with 5 cm scale mark.

FG 73-2

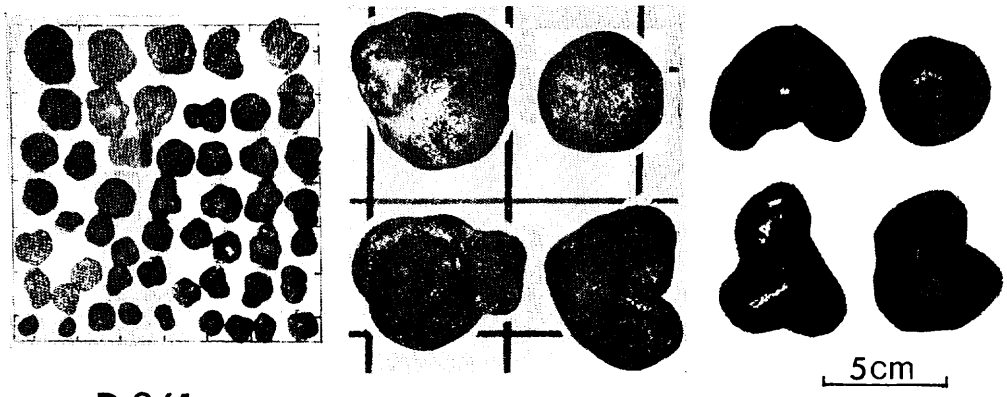

D 261

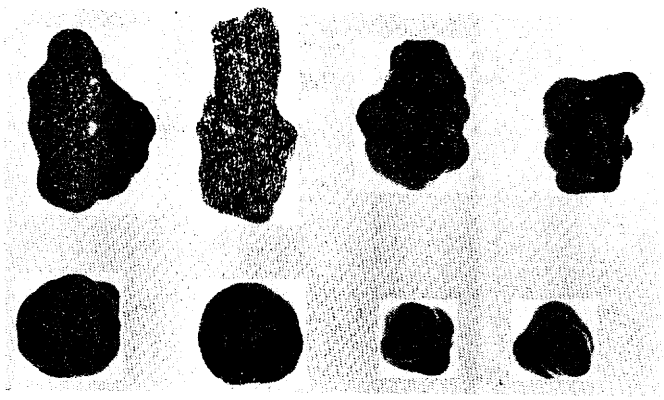

ST 1037 FG 74-1

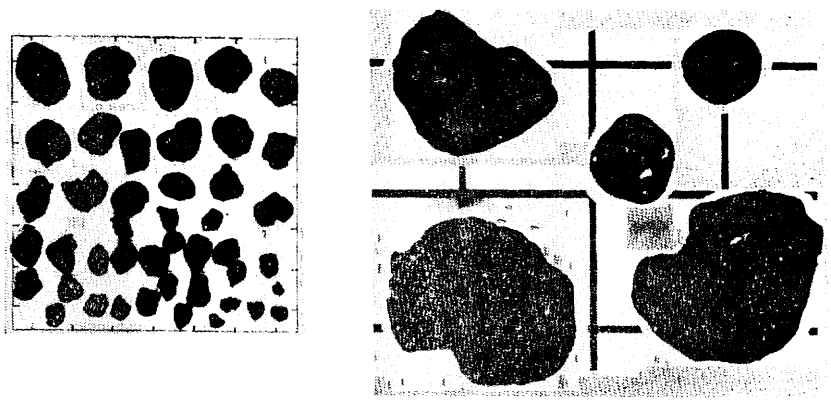

(2)

FG 74-1

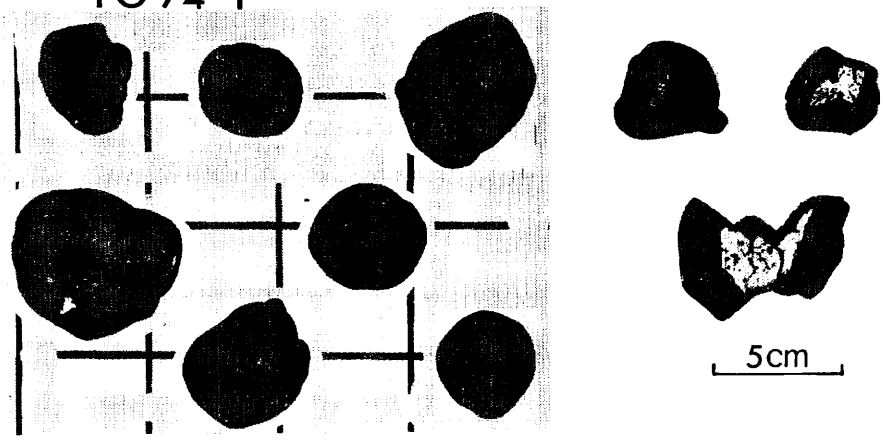

FG74-2

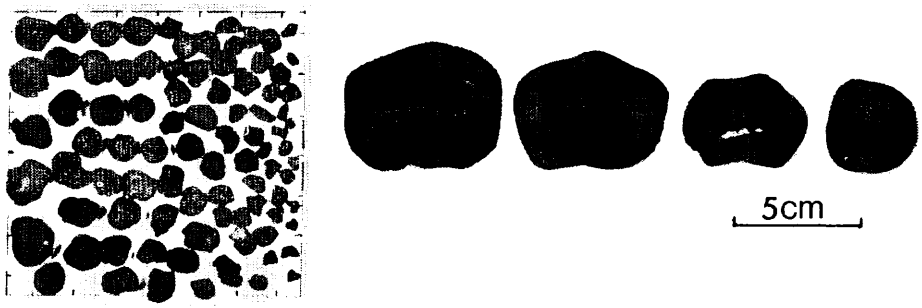

ST 1037-1 G(B)605-1

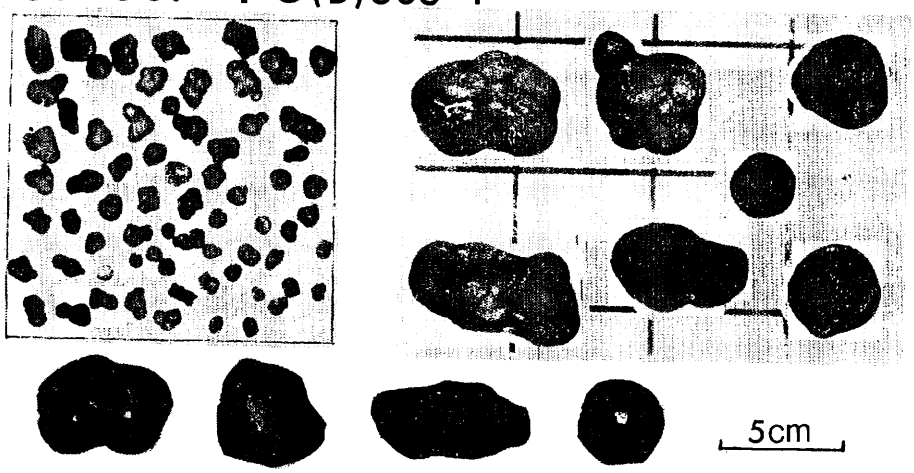

ST 1038 FG 75-1

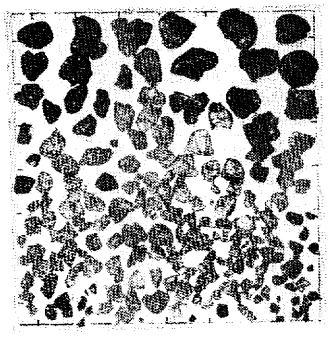

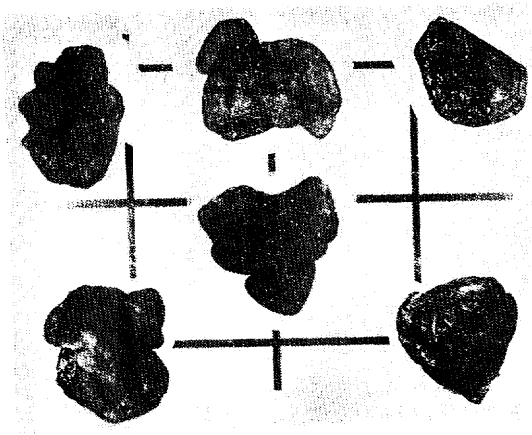

FG 75-2

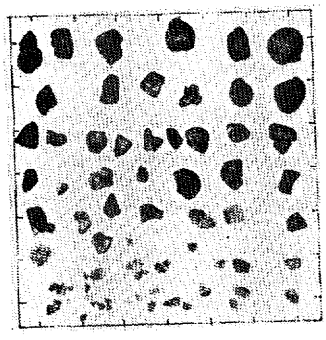

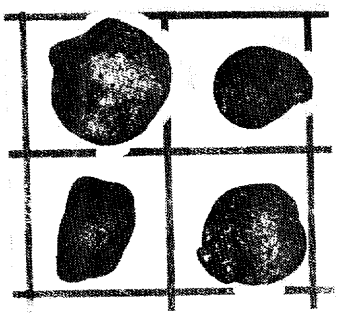

ST 1038-A FG 113-1

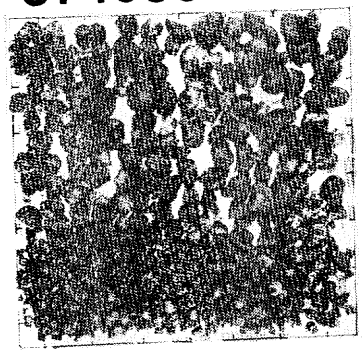

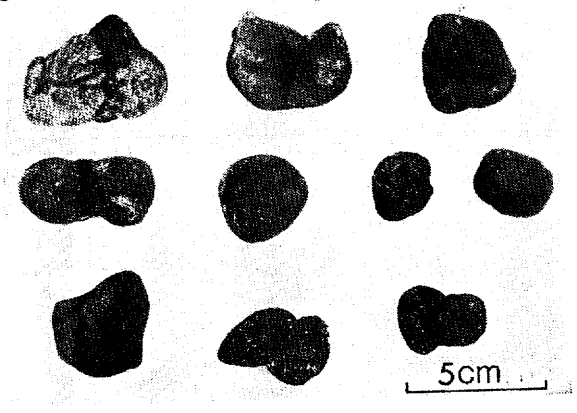

(4)

FG 113-2

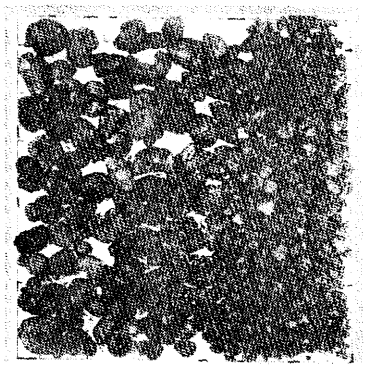

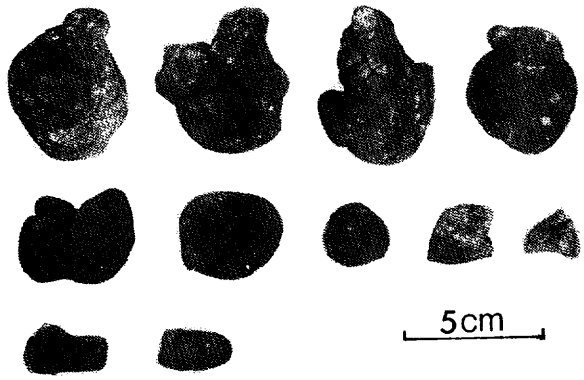

G640

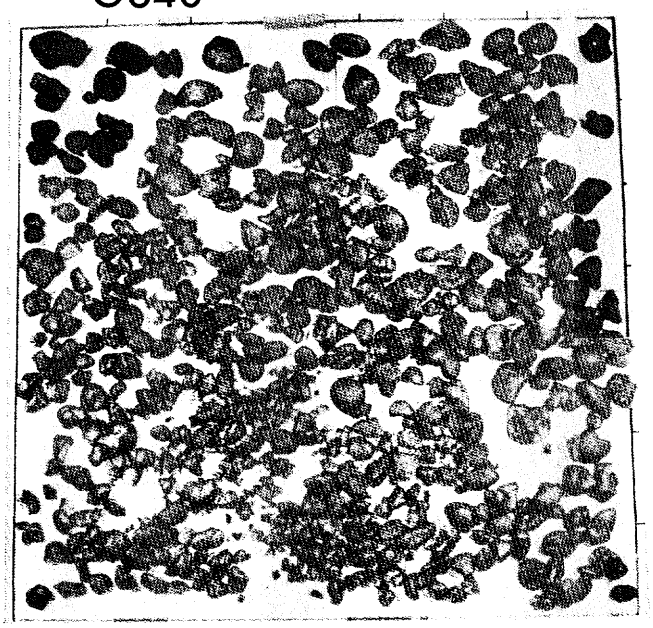

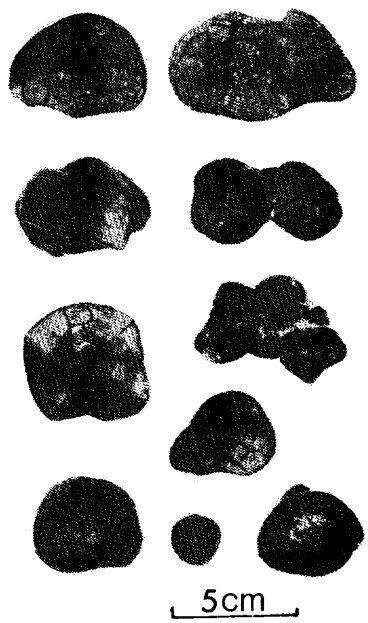

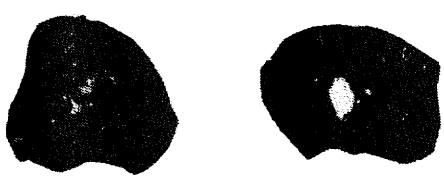

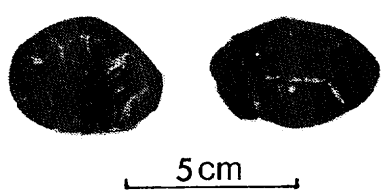

(5)

ST1039 FG76-1

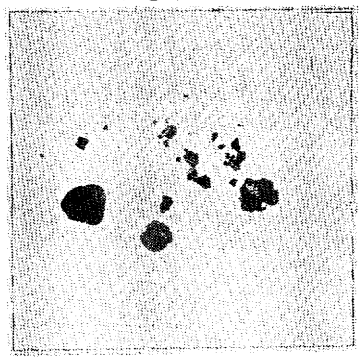

ST1039-A G641

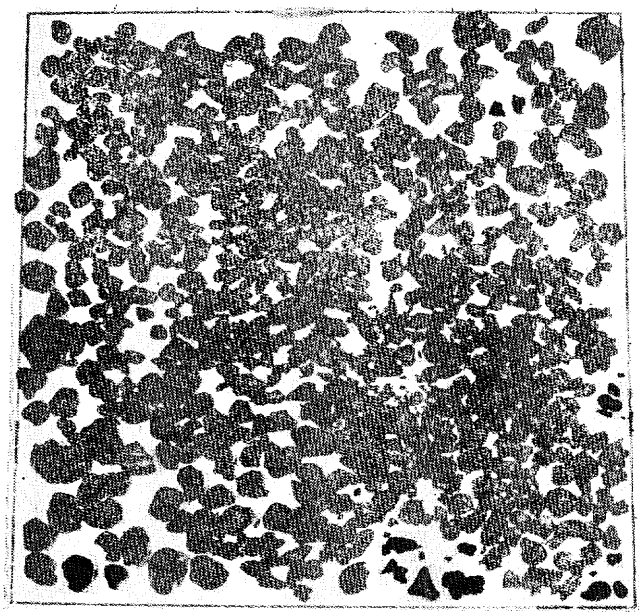

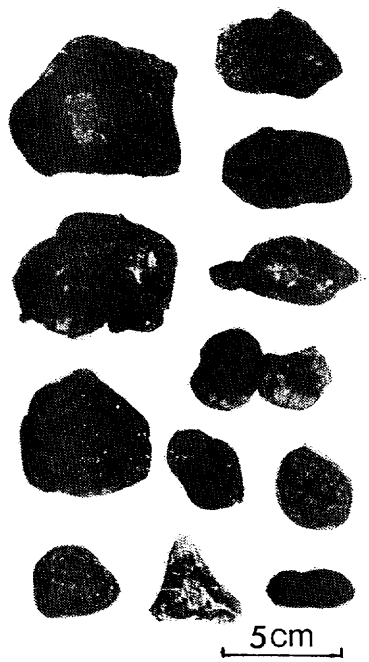

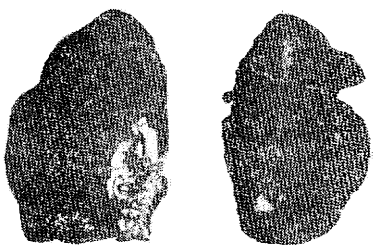

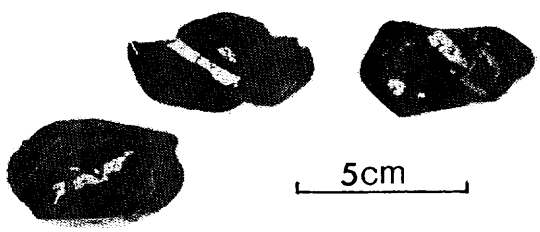

(6)

FG114-1

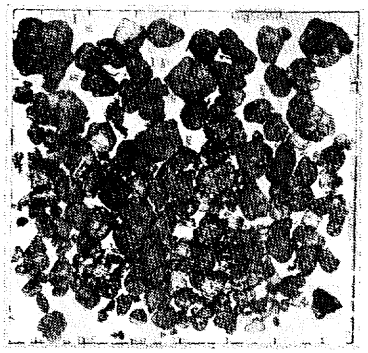

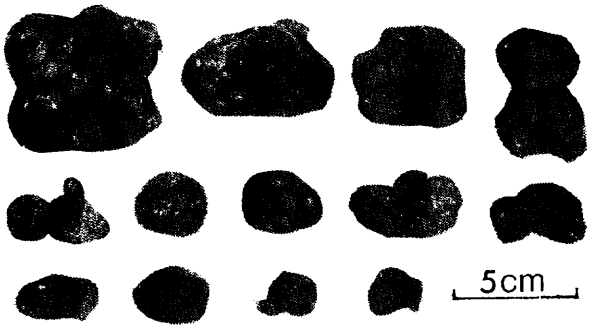

FG114-2

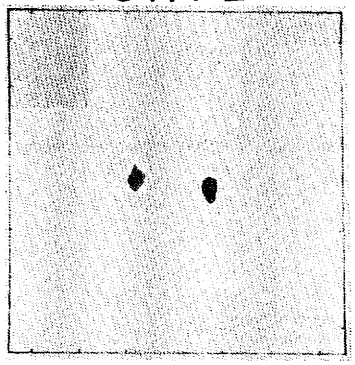

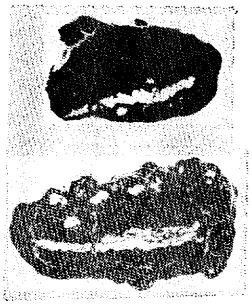

ST 1040 G(B)608

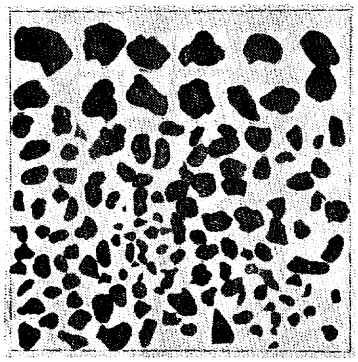

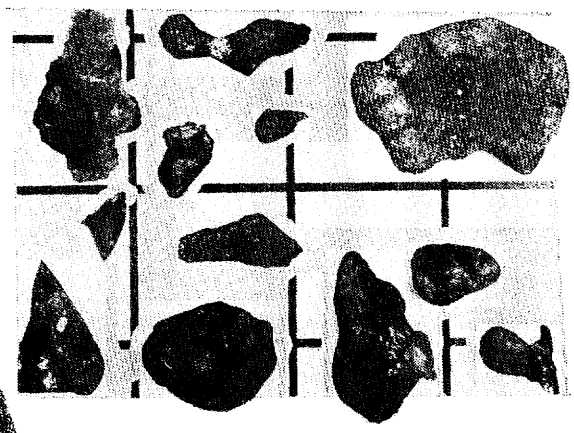

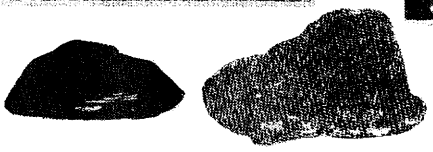

ST 1041 G(B)609

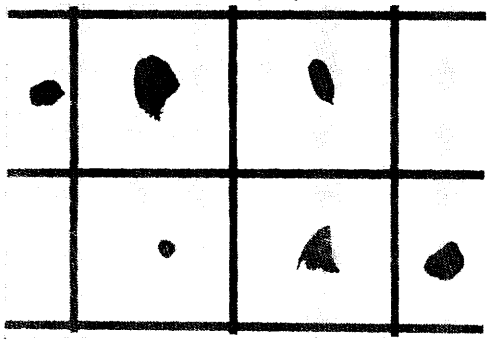

FG78-1

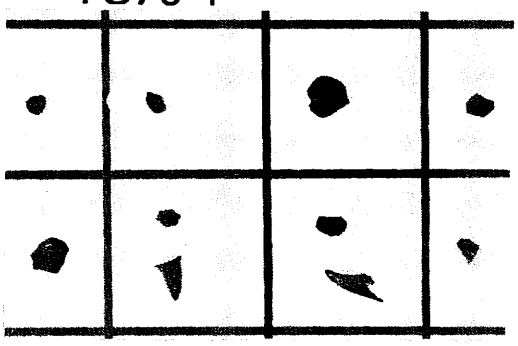

FG78-2

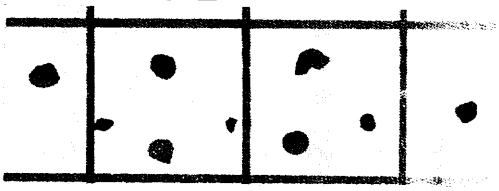

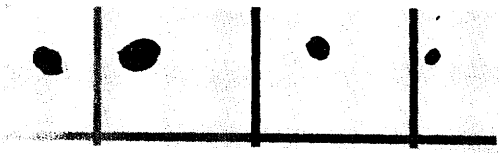

ST1042 G(B)610

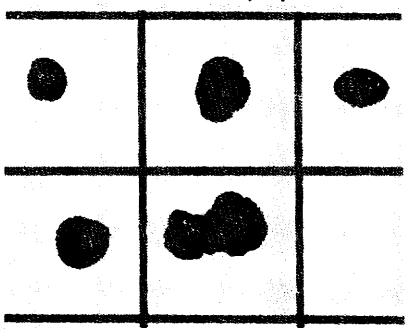

FG79-1

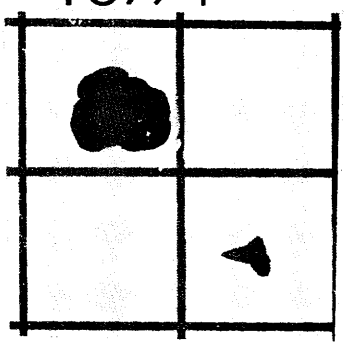

FG79-2

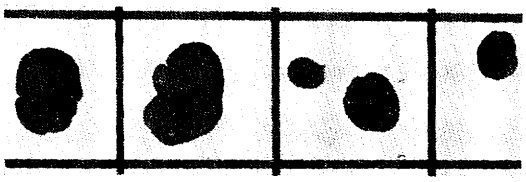

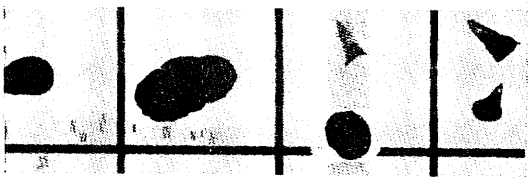

(8)

ST 1043 G611

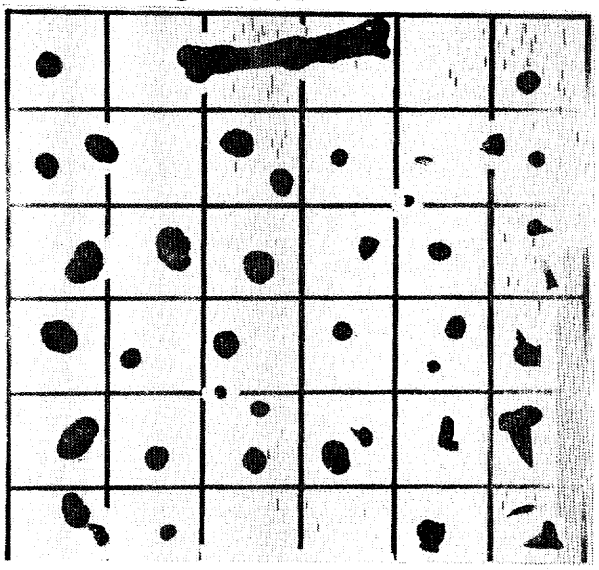

FG80-1

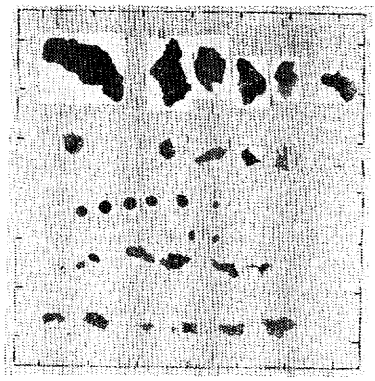

FG80-2

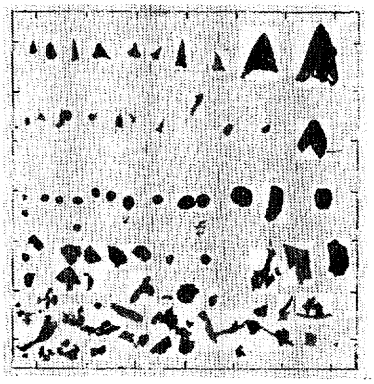

ST 1044 FG81-1

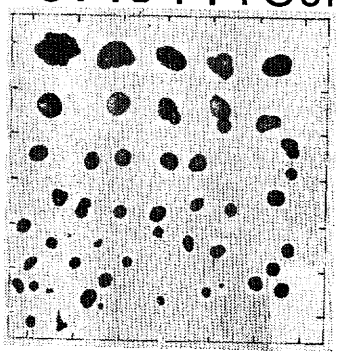

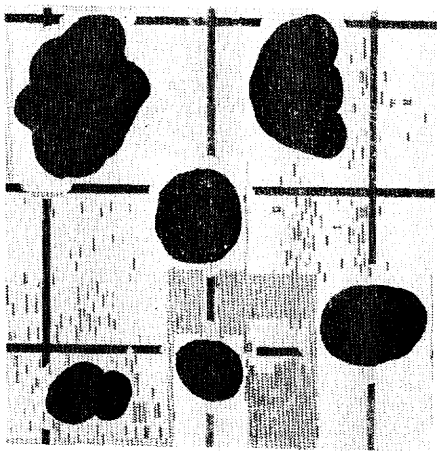

(9)

FG 81-2

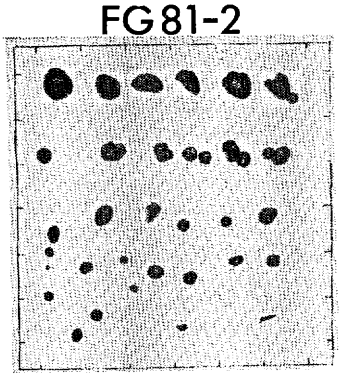

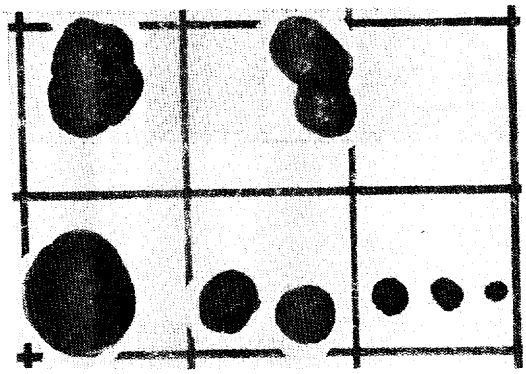

ST 1044-1 G612-1

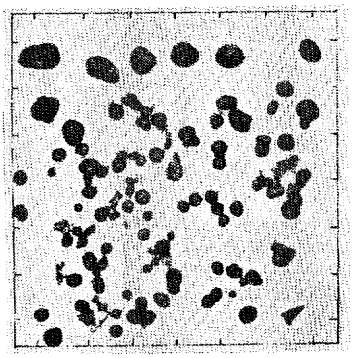

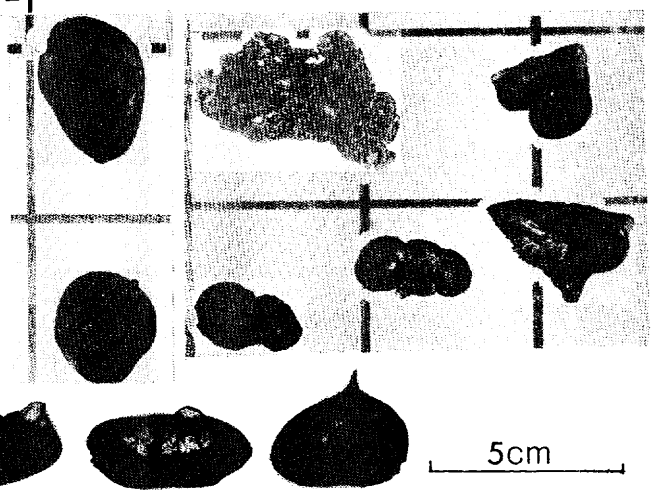

5cm

ST 1045 G613

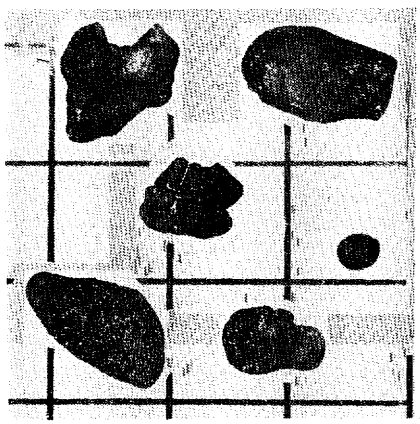

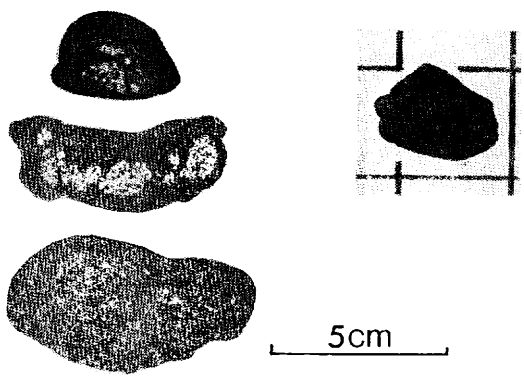

5cm

ST 1047 G615

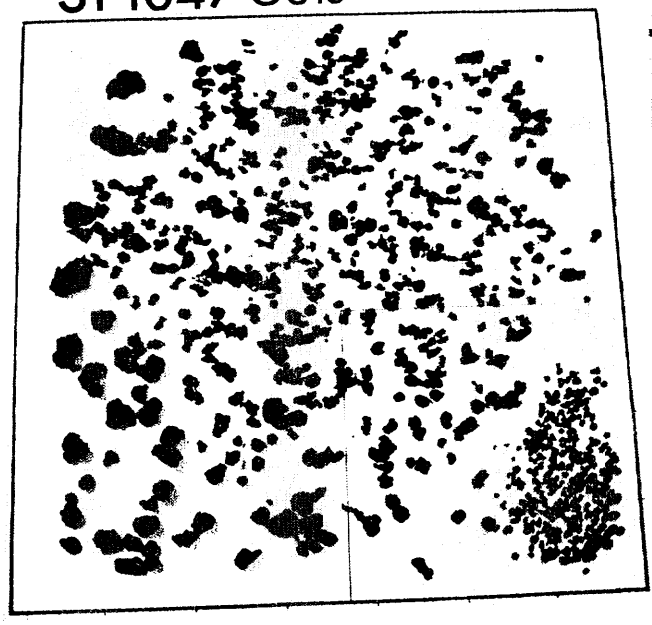

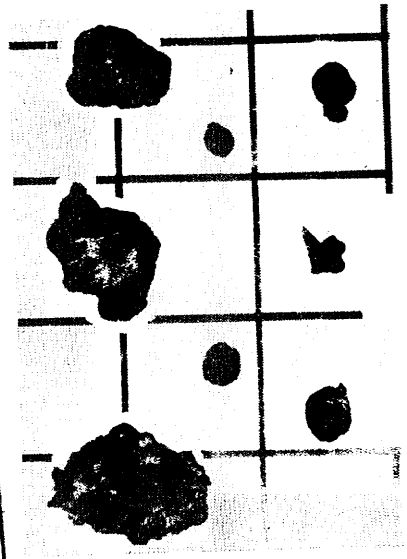

FG84-1

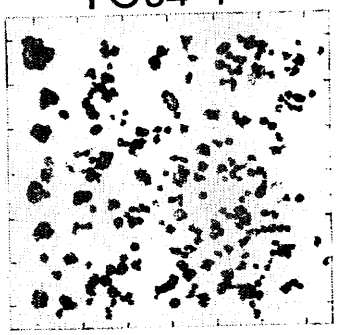

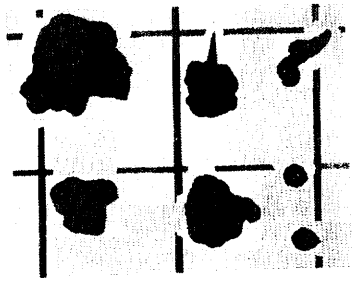

FG84-2

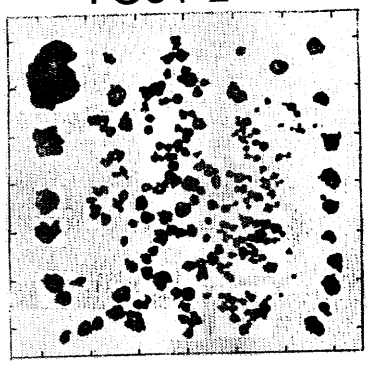

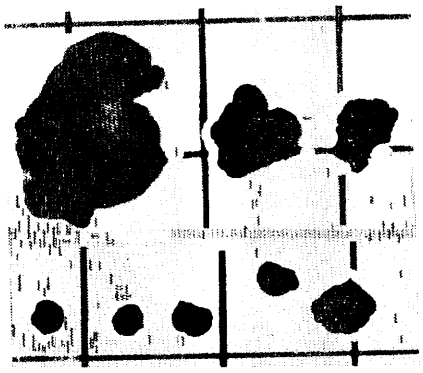

(11)

ST 1048 G(B)616

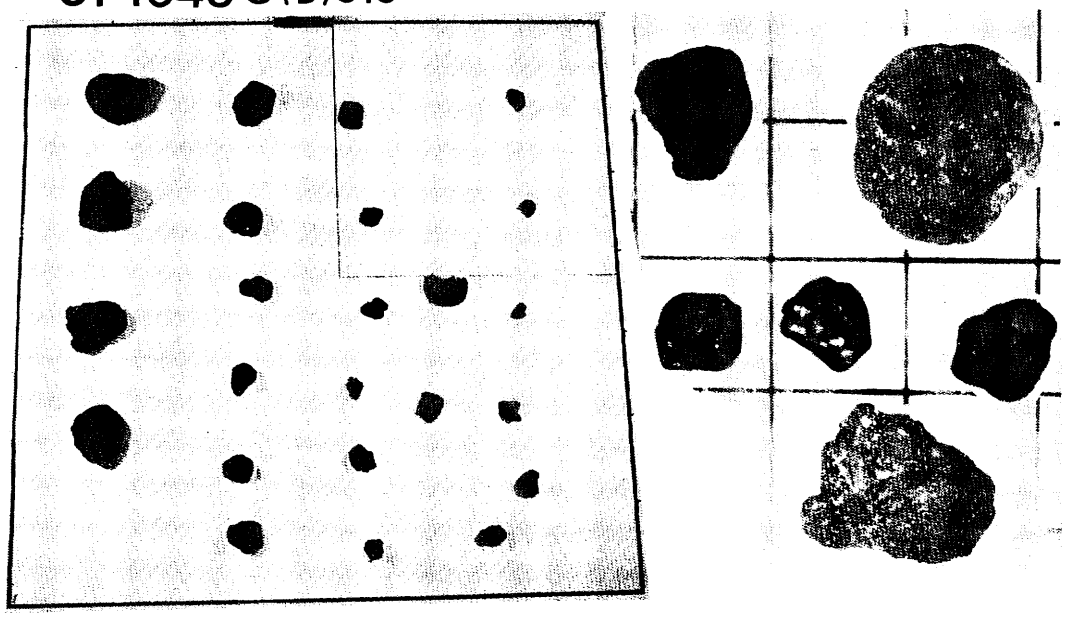

FG 85-1

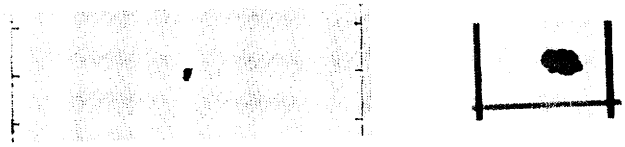

FG 85-2

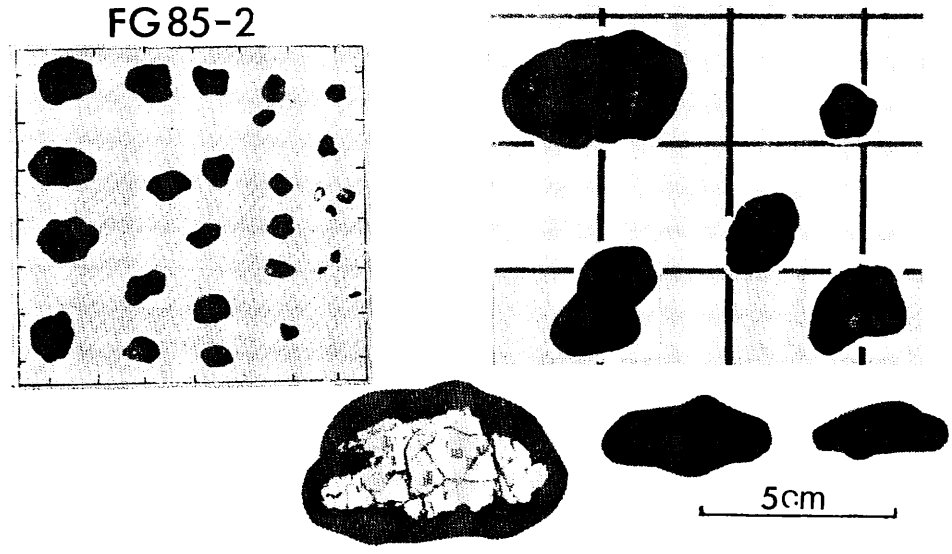

ST 1046 G614

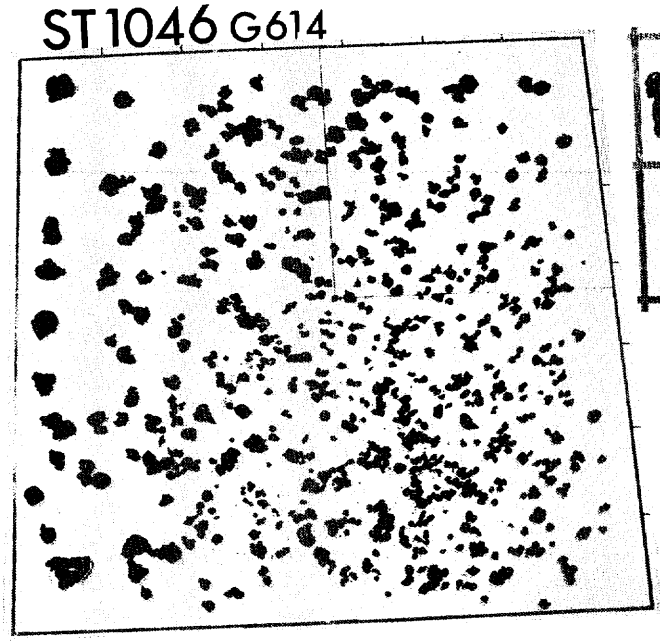

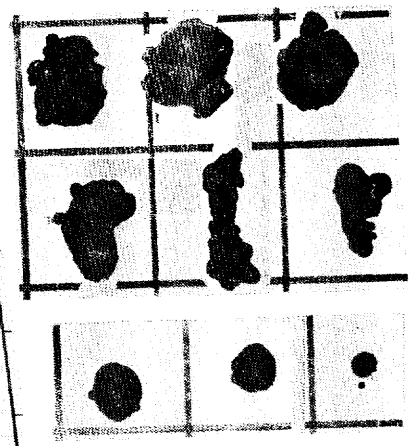

FG 83-1

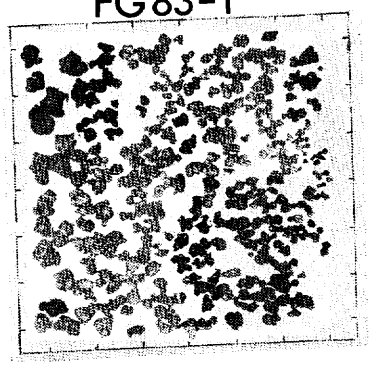

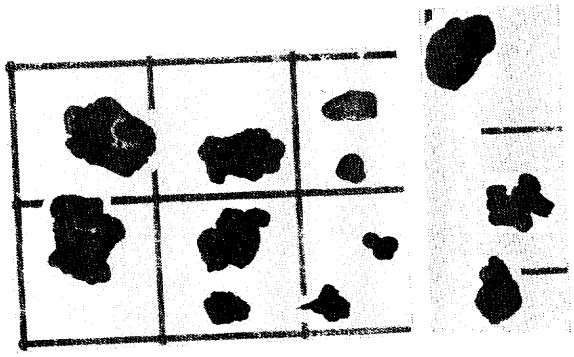

FG 83-2

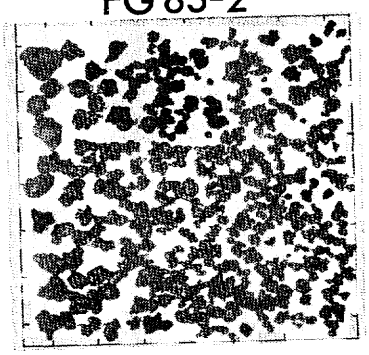

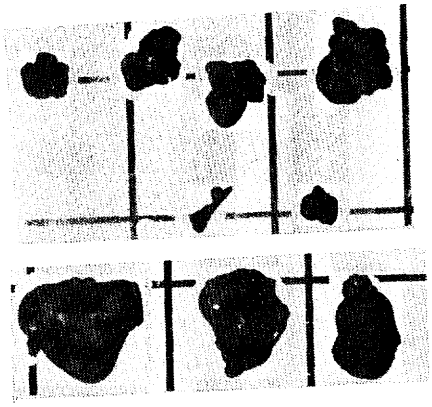

ST 1048-1 G616

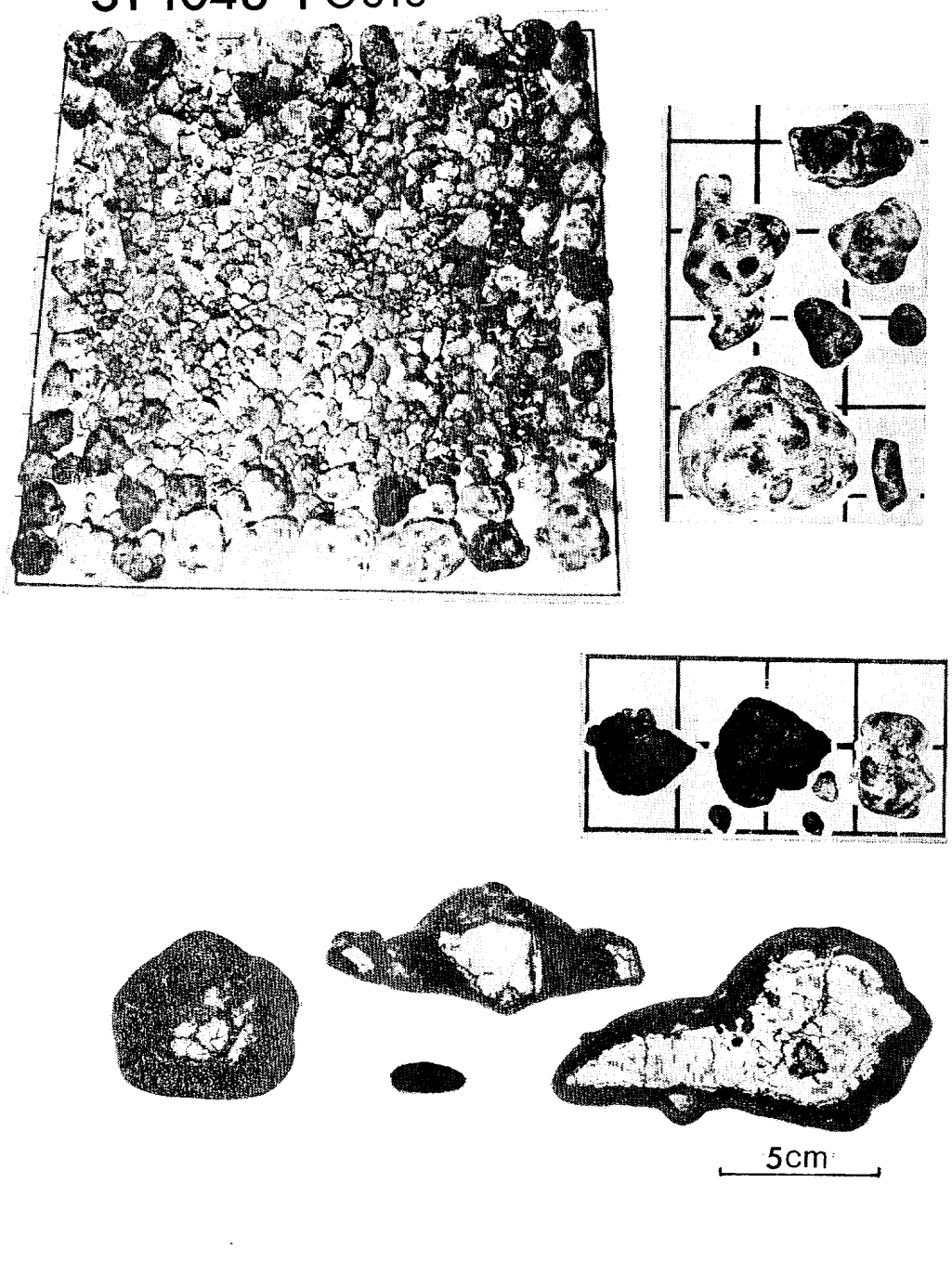

(14)

ST 1049 G617

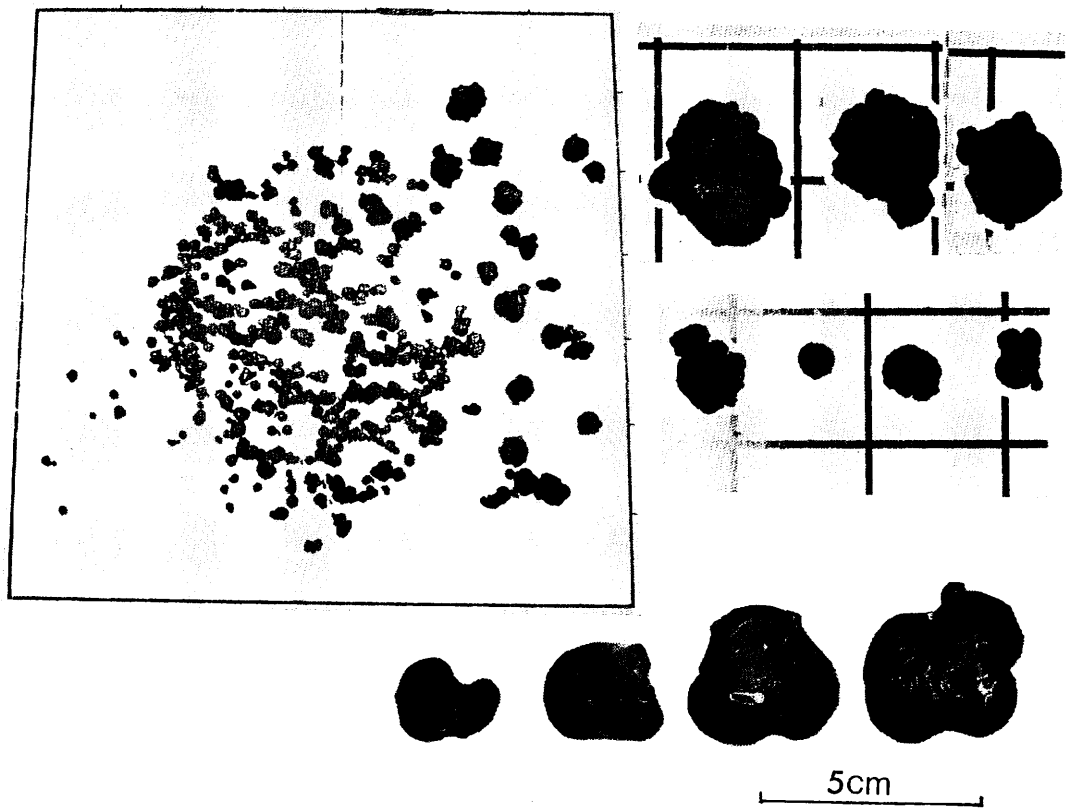

FG86-1

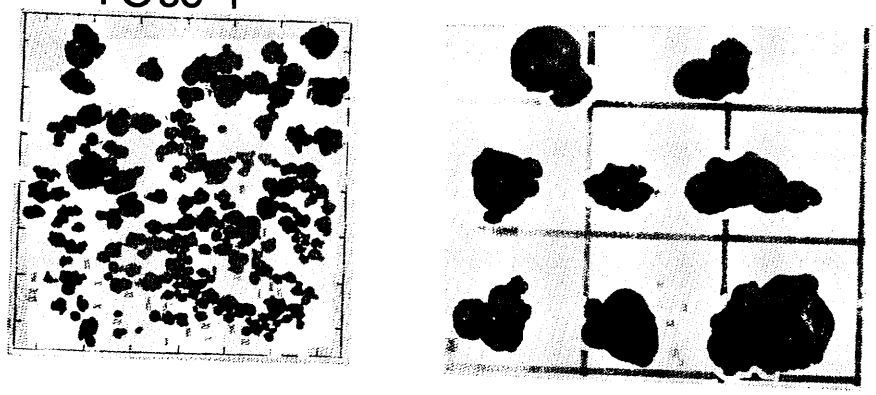

(15)

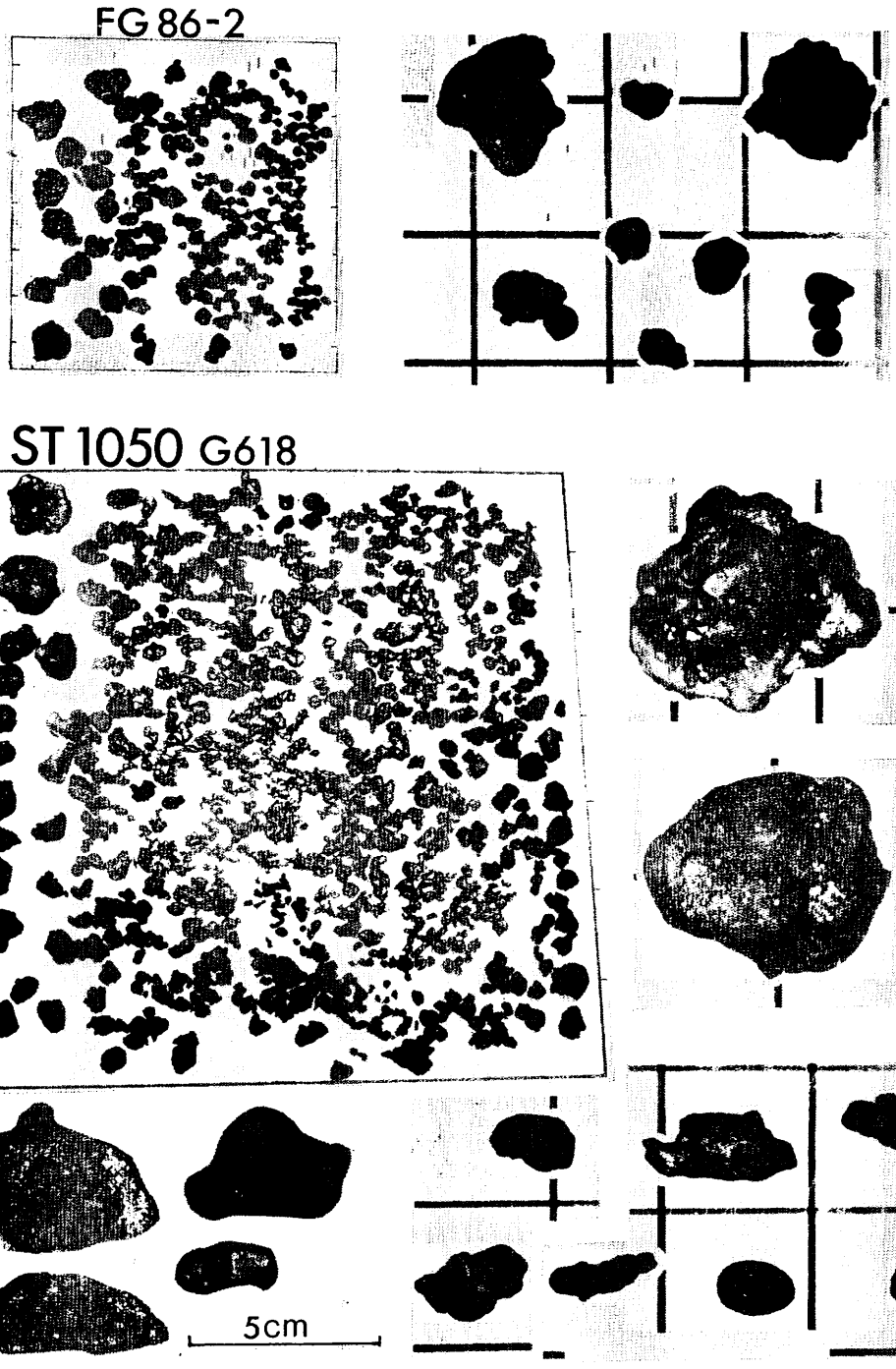

(16)

ST 1050 FG87-1

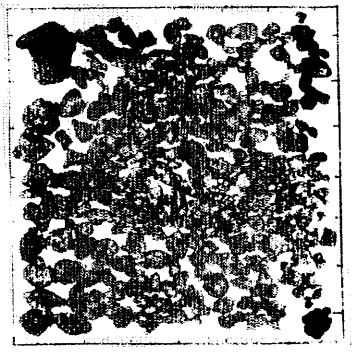

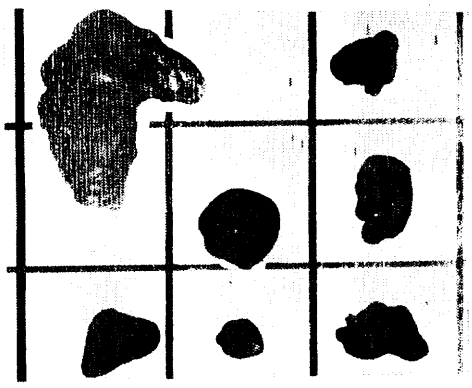

FG87-2

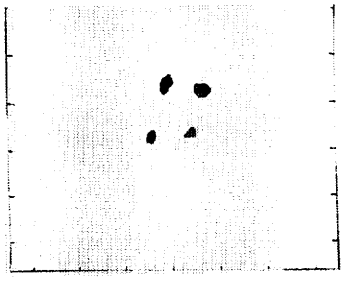

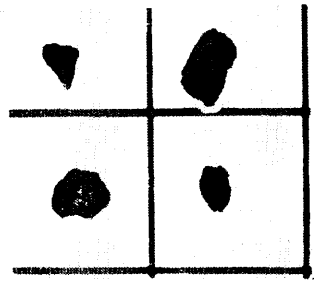

ST 1051 G619

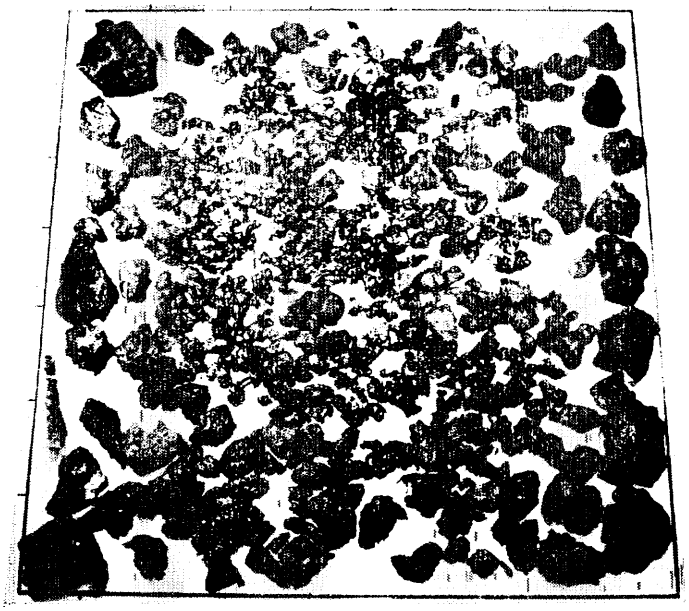

G619

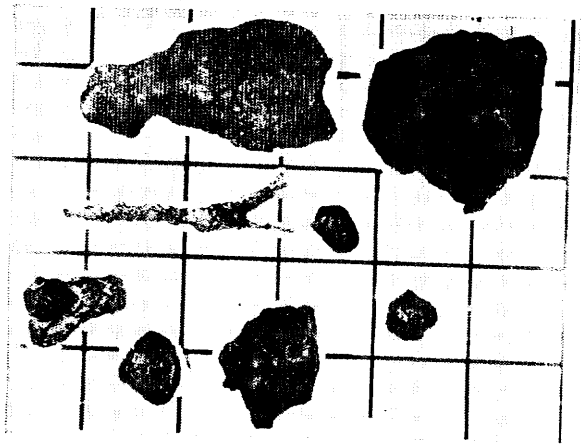

5cm

FG88-1

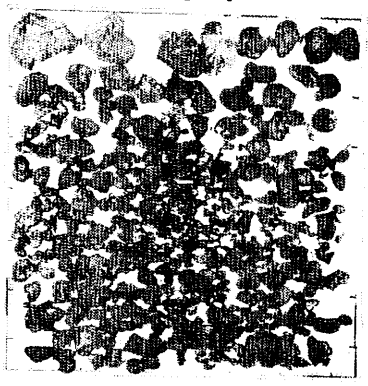

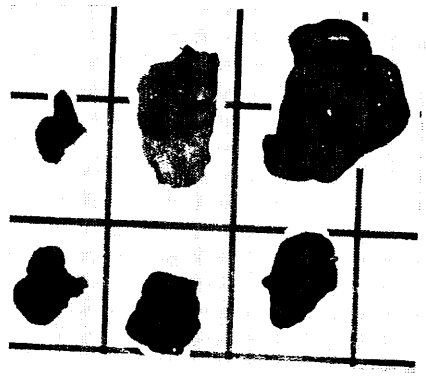

FG88-2

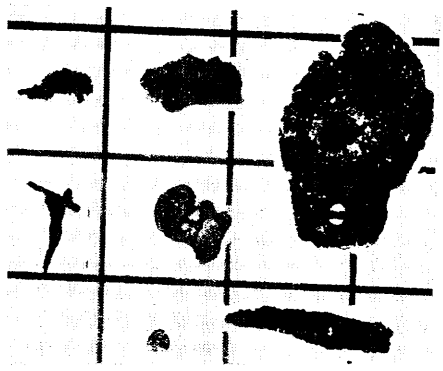

(18)

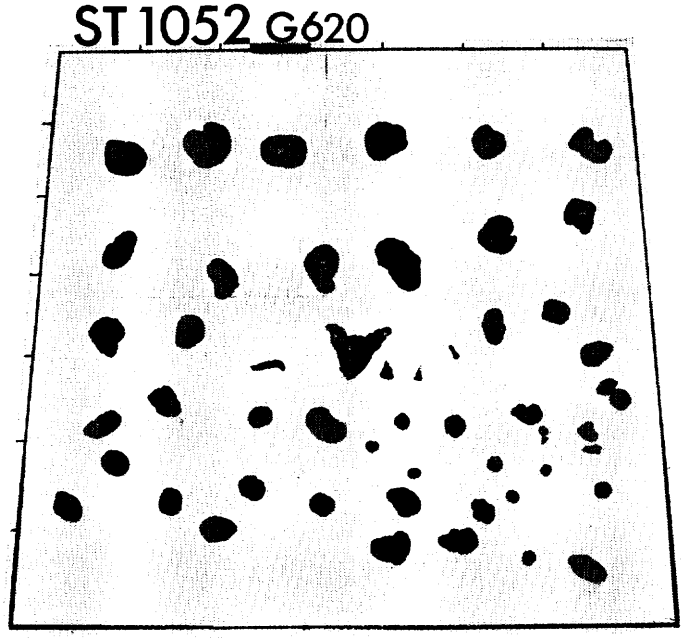

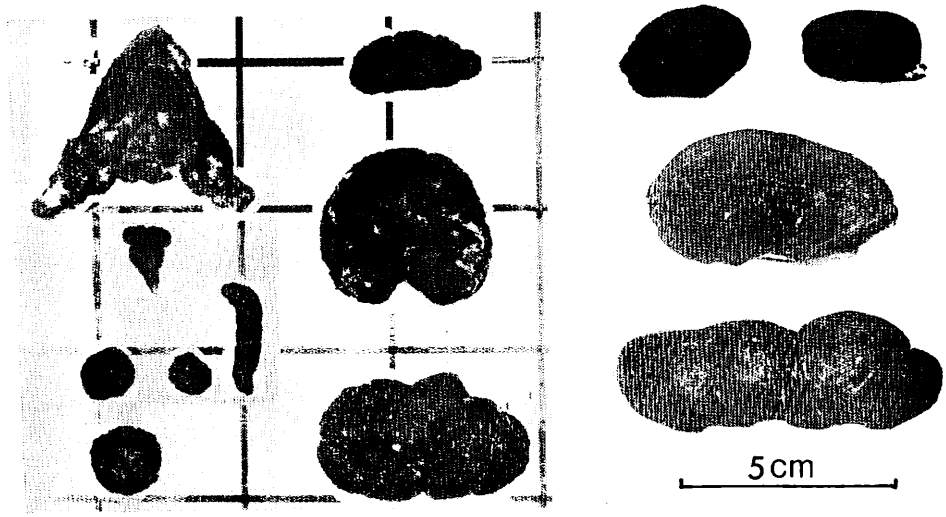

(19)

ST 1052 FG89-1

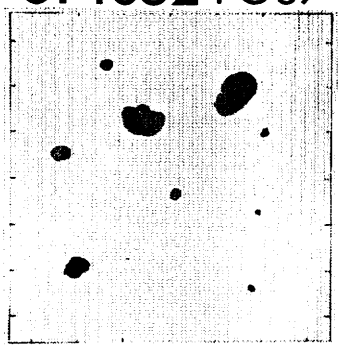

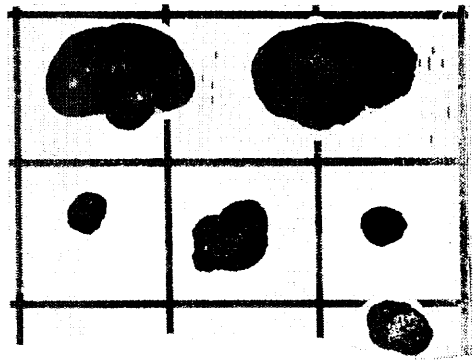

FG89-2

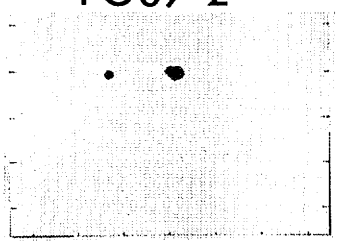

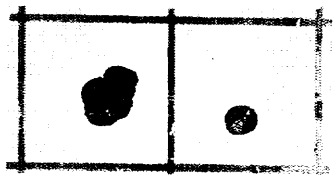

ST 1053 G621

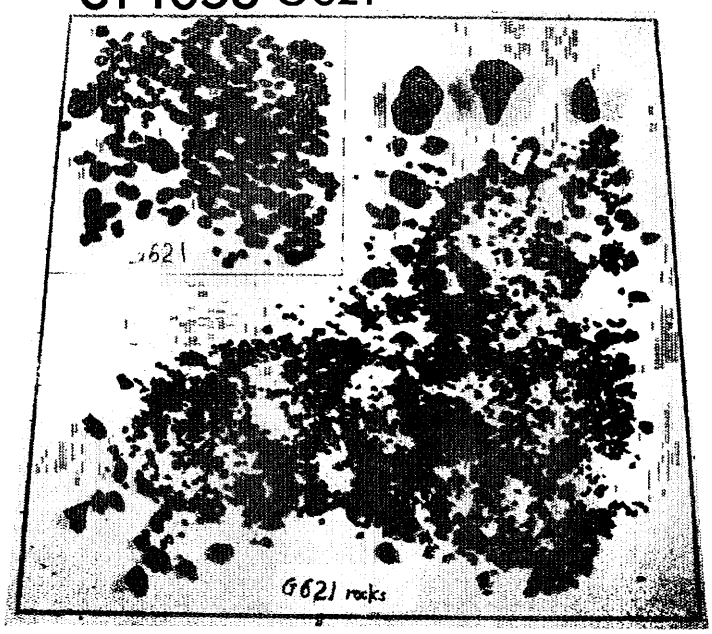

ST 1053 G621

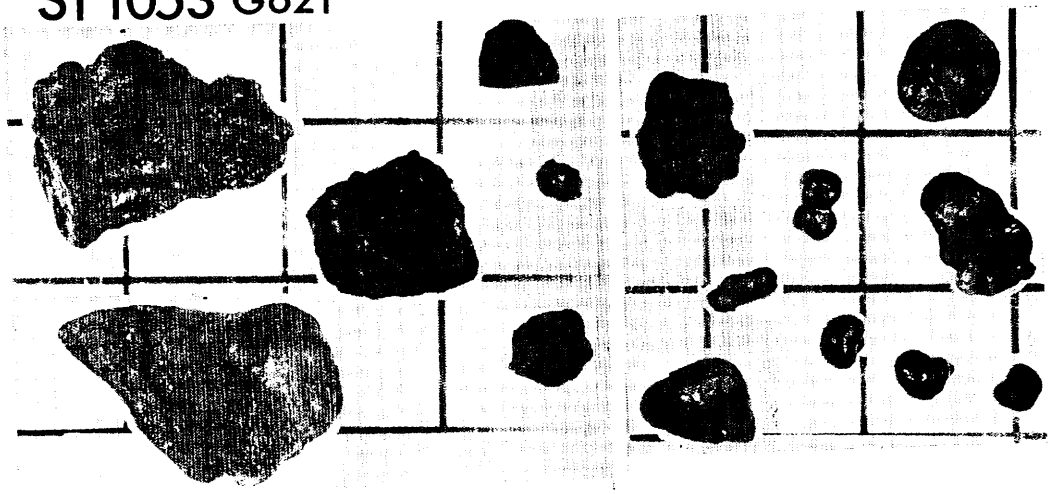

FG90-1

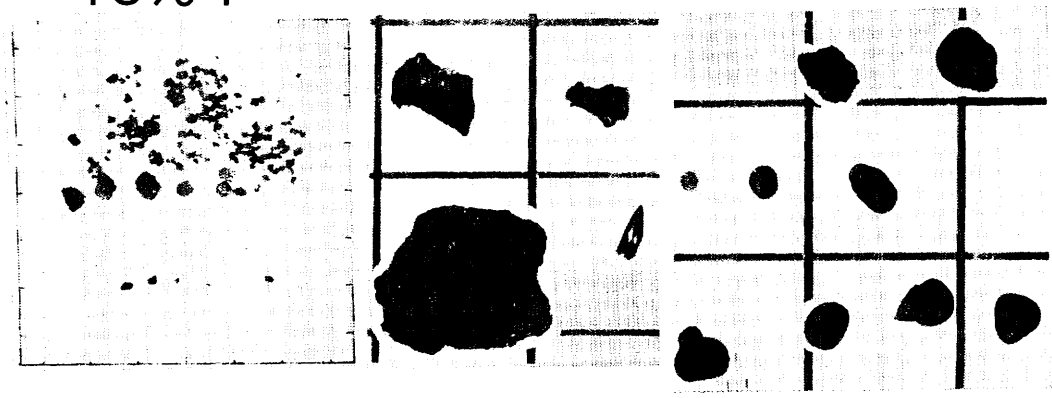

FG90-2

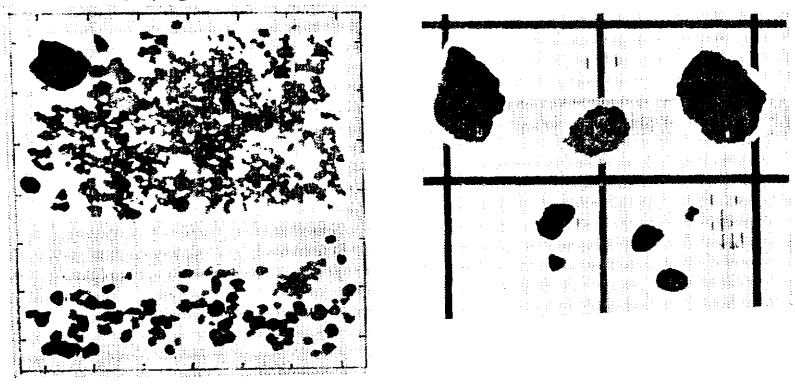

(21)

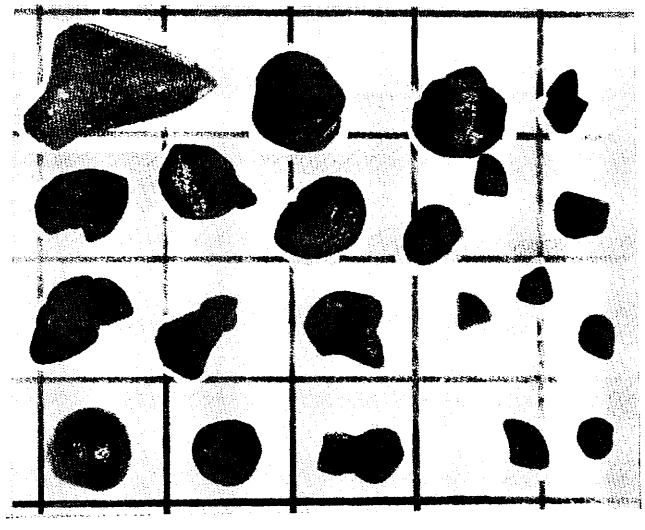

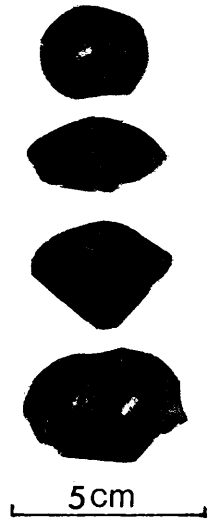

(22)

ST 1054 FG91-2

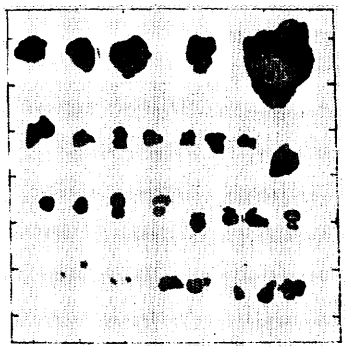

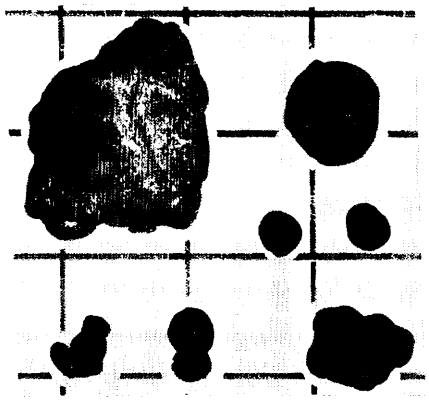

ST 1055 G(B)625

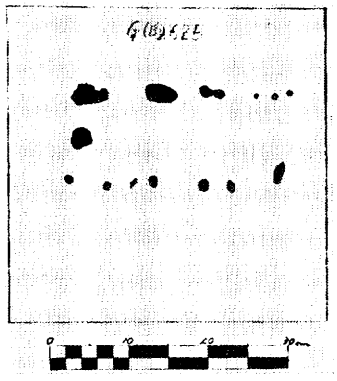

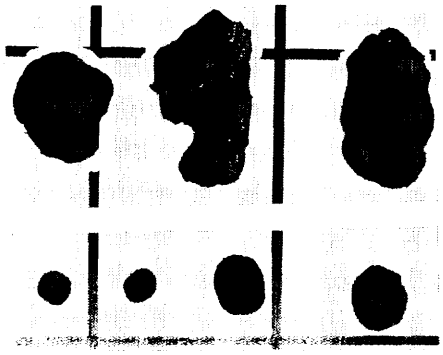

FG94-1

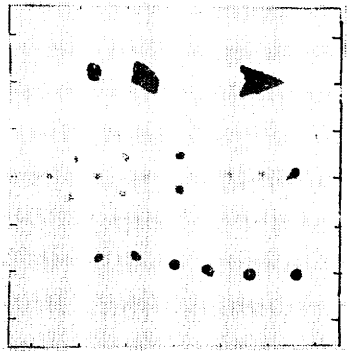

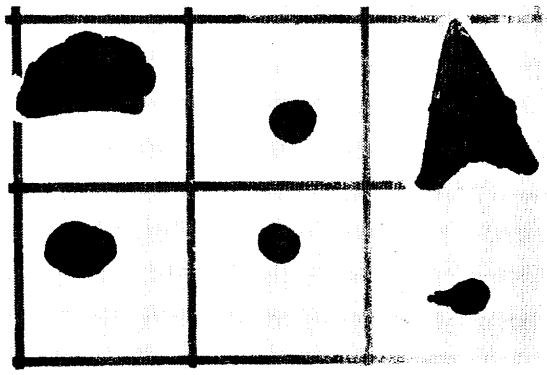

(23)

ST 1055 FG94-2

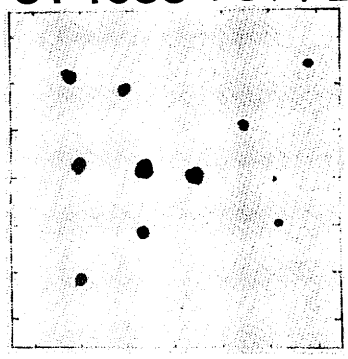

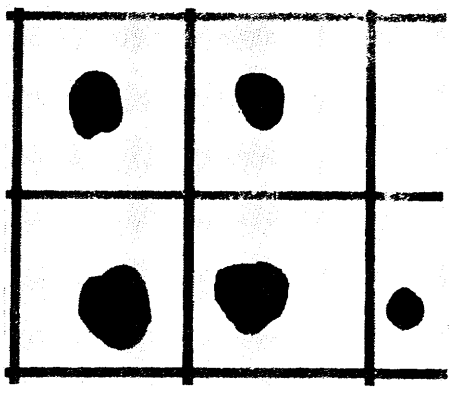

ST 1056 G(B)626

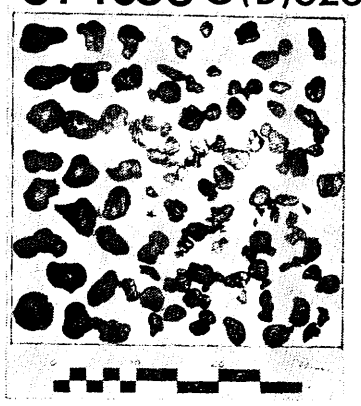

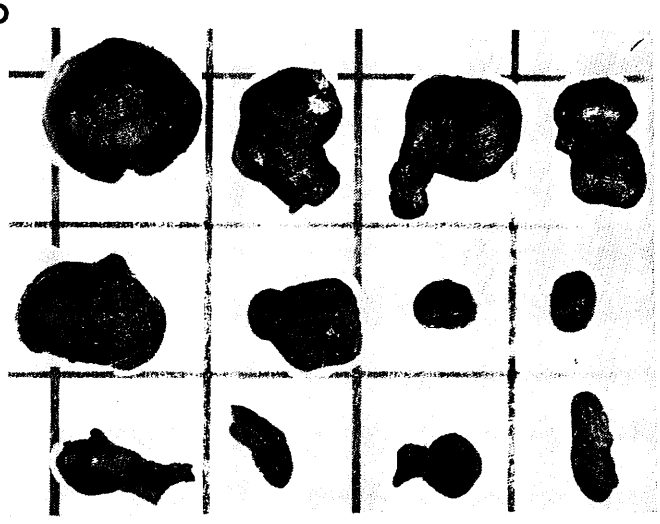

5cm

(24)

ST 1057 FG96-1

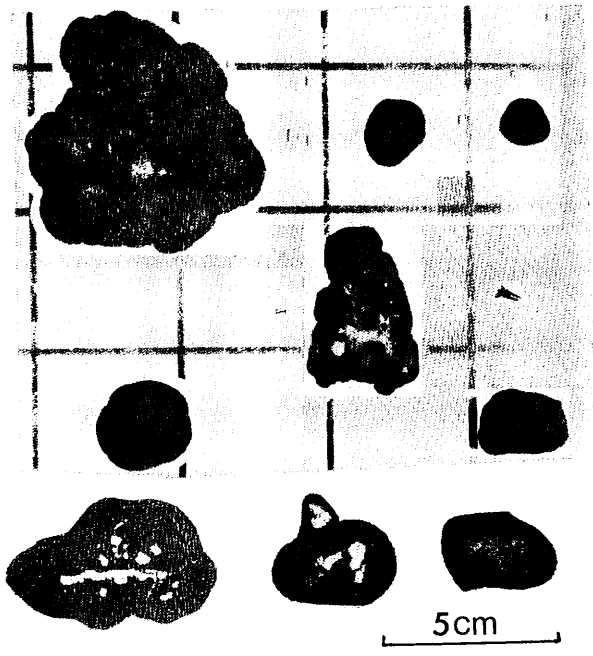

FG96-2

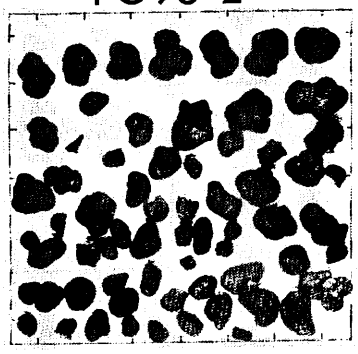

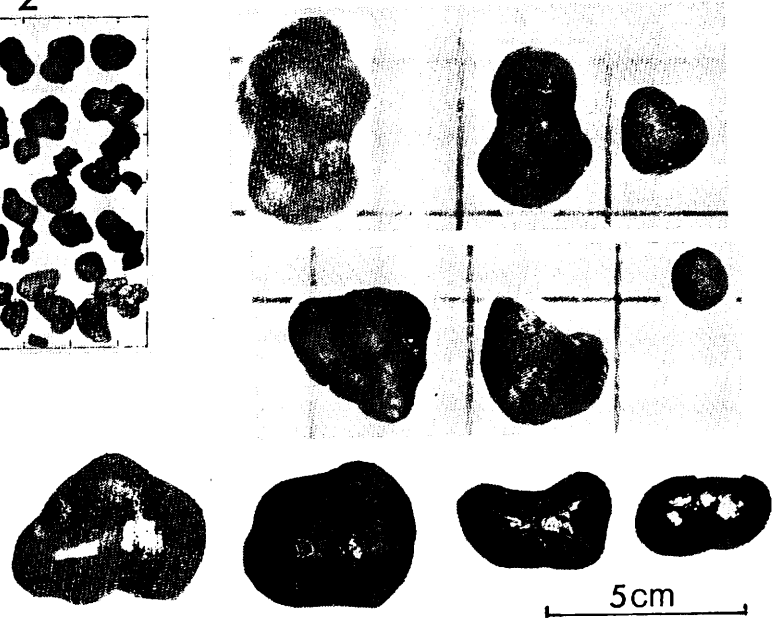

(25)

ST 1056 FG95-1

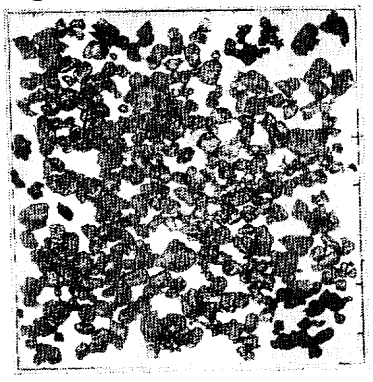

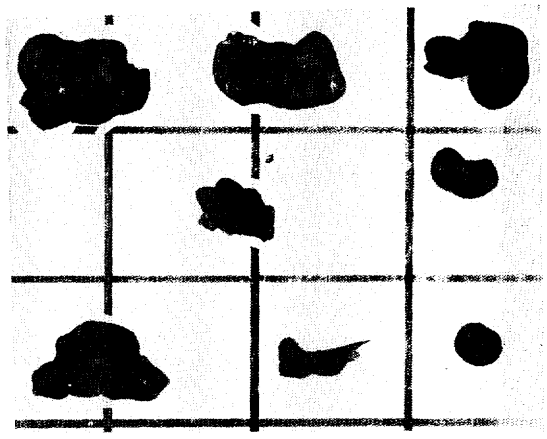

FG95-2

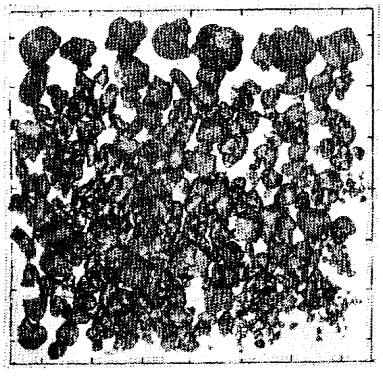

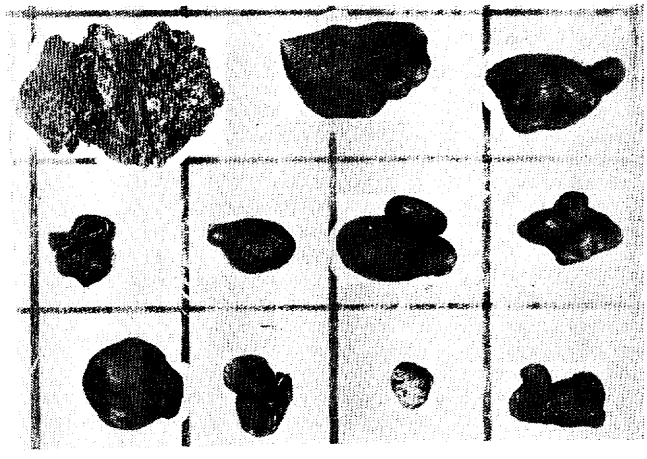

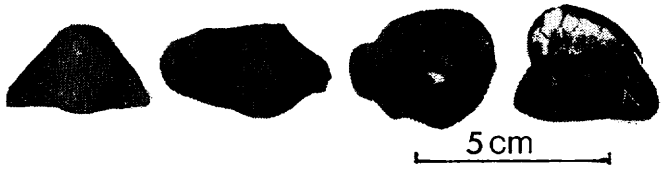

(26)

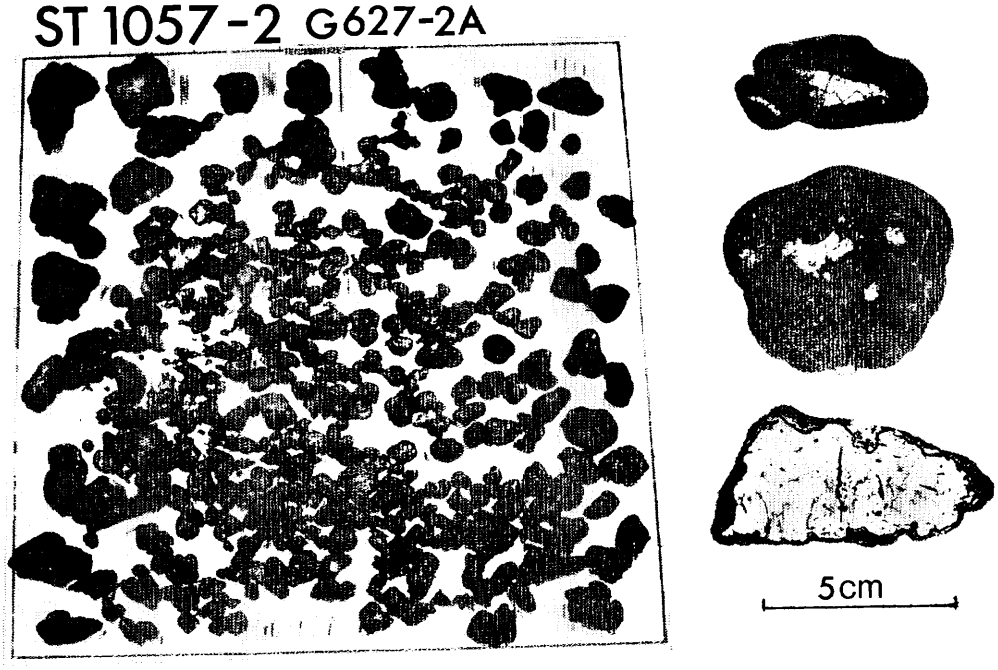

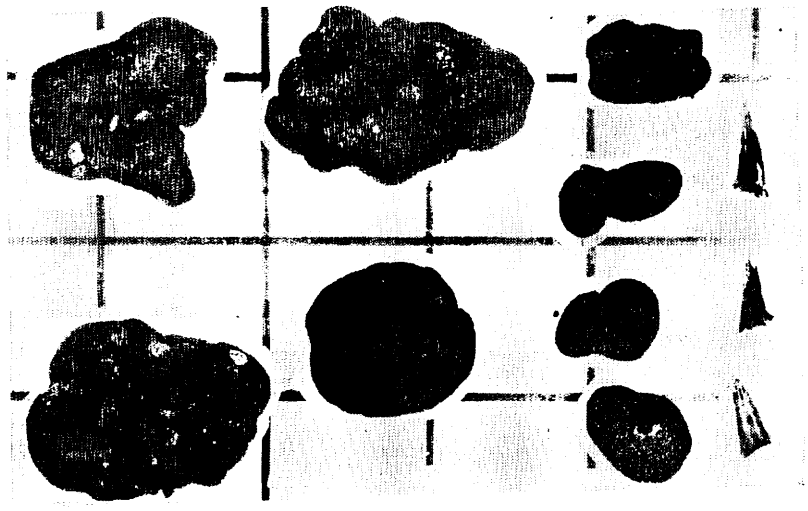

(27)

ST 1057-2 G627-2B

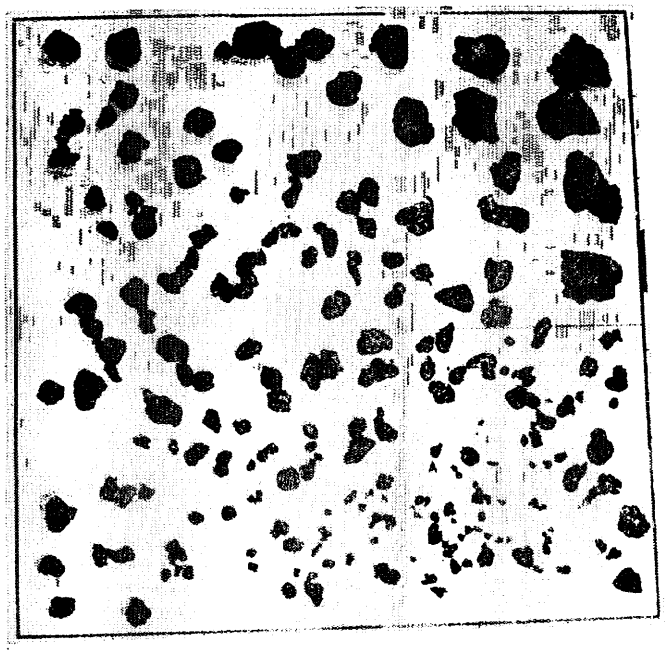

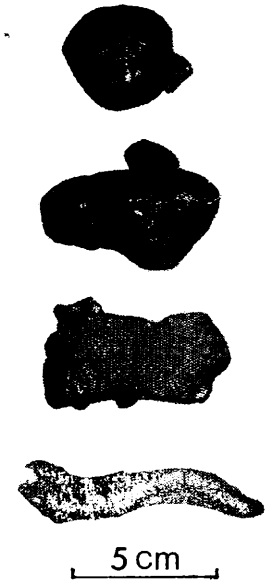

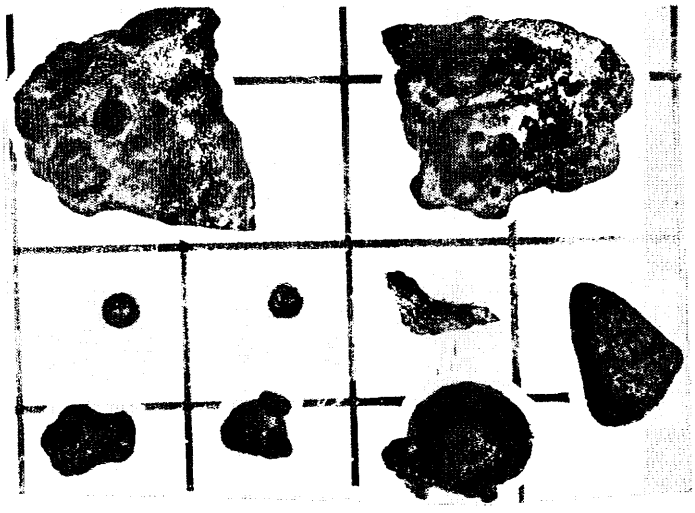

(28)

ST 1059 G629

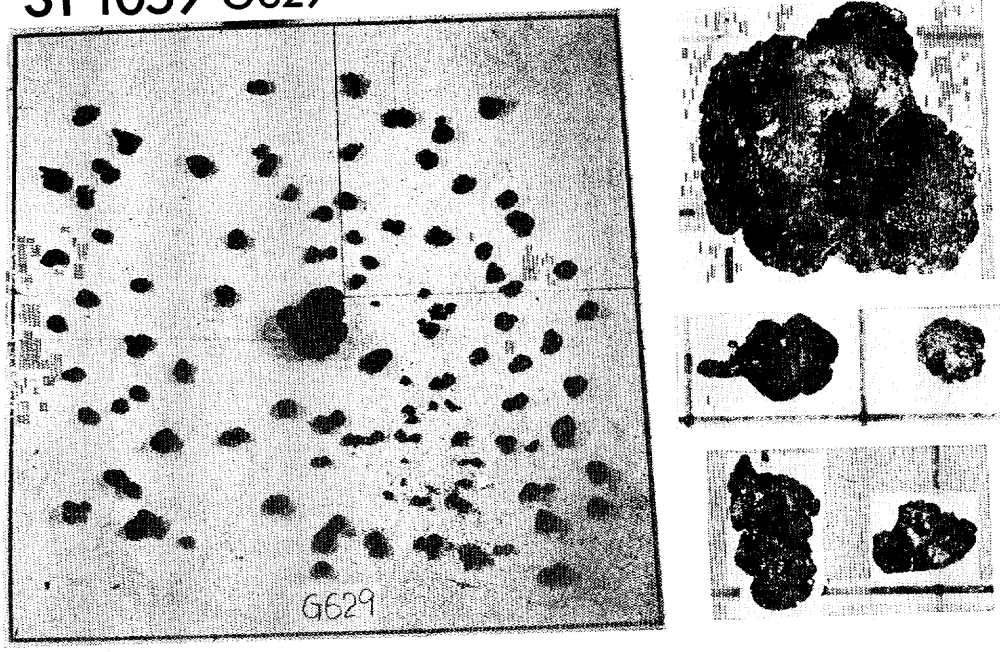

FG98-1

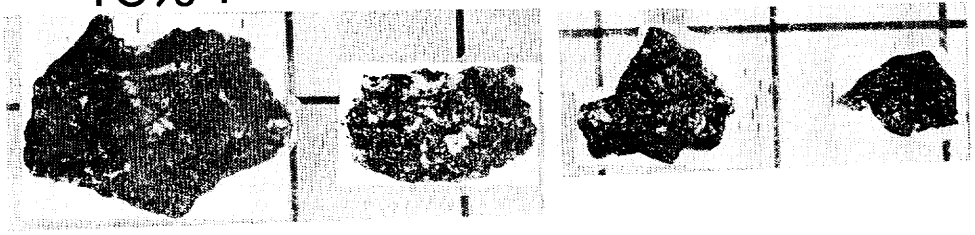

FG98-2

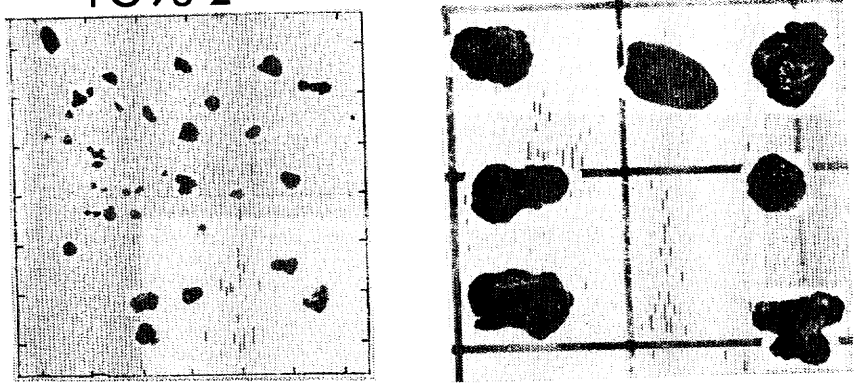

(29)

ST 1076 FG112-1

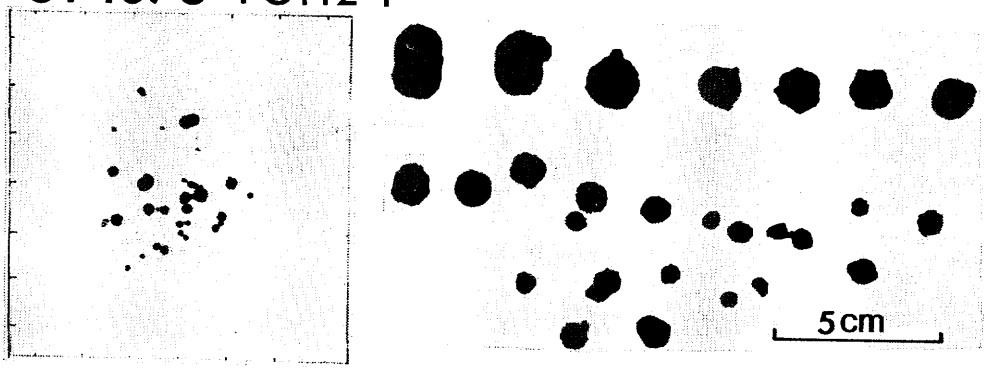

FG112-2

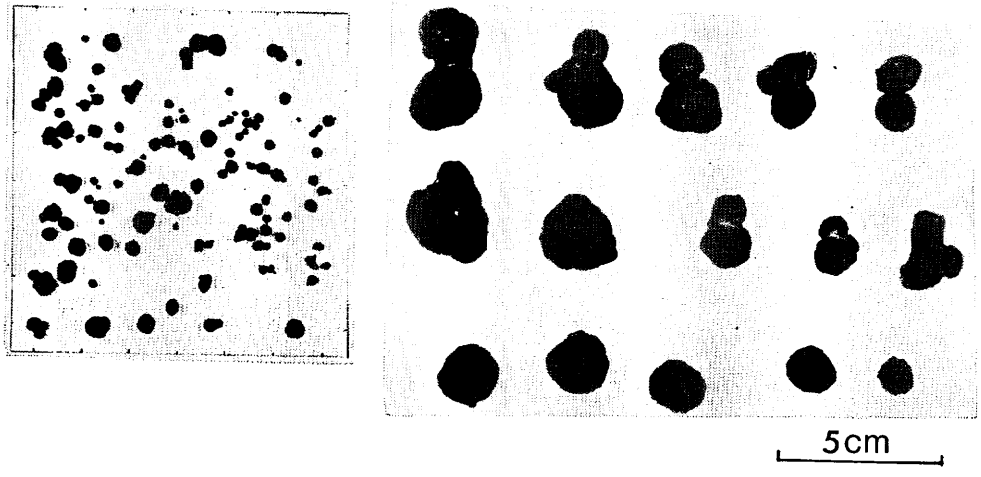

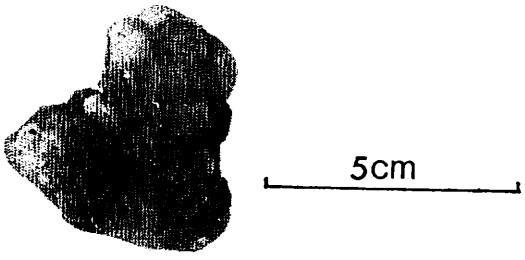

(30)

ST 1074 FG110-1

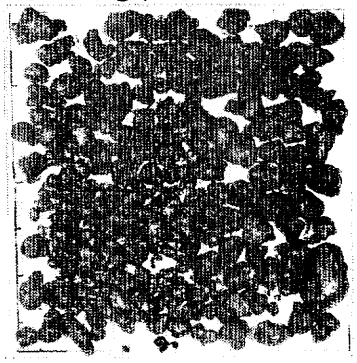

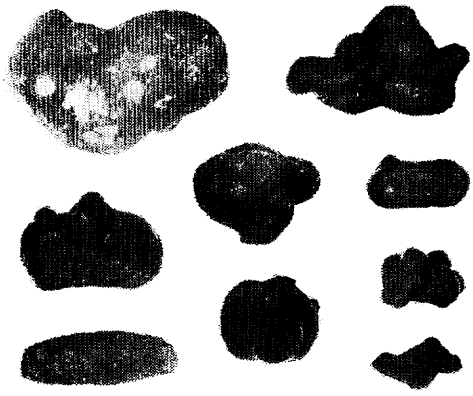

5cm

FG110-2

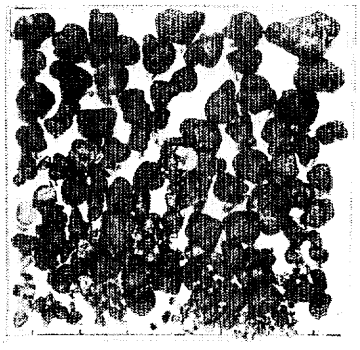

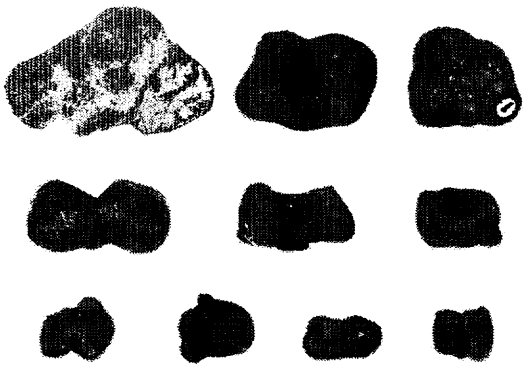

5cm

ST 1073 FG109-7

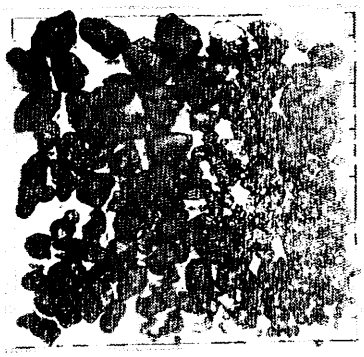

FG109-8

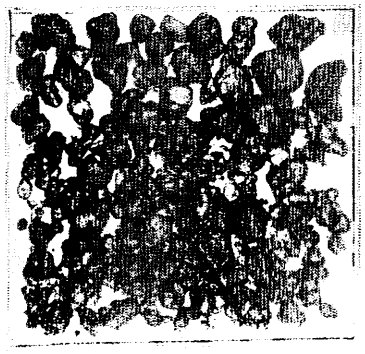

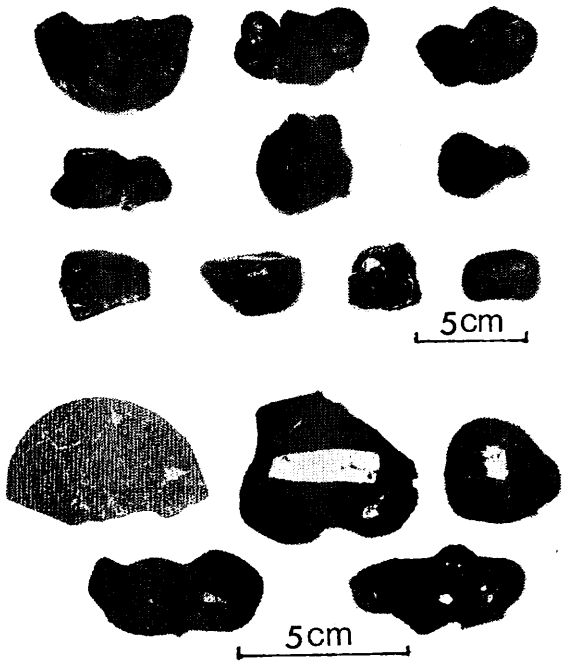

(32)

ST 1073 FG109-5

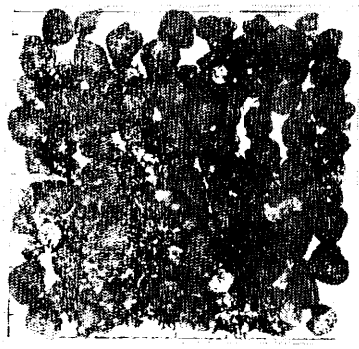

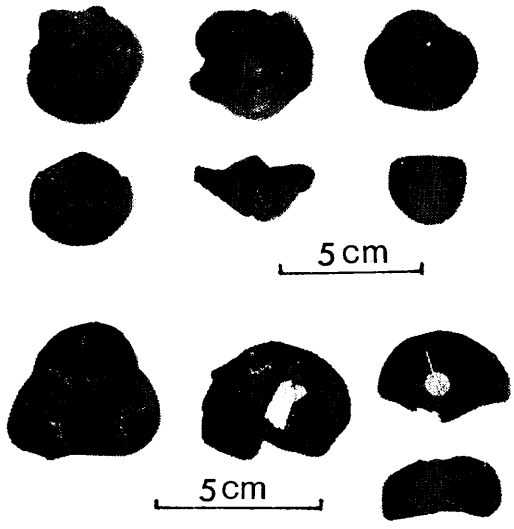

FG109-6

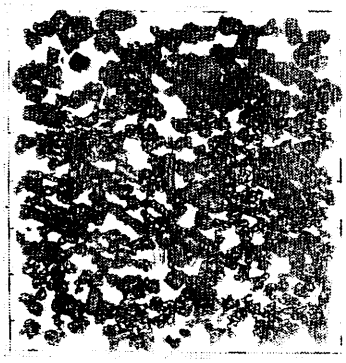

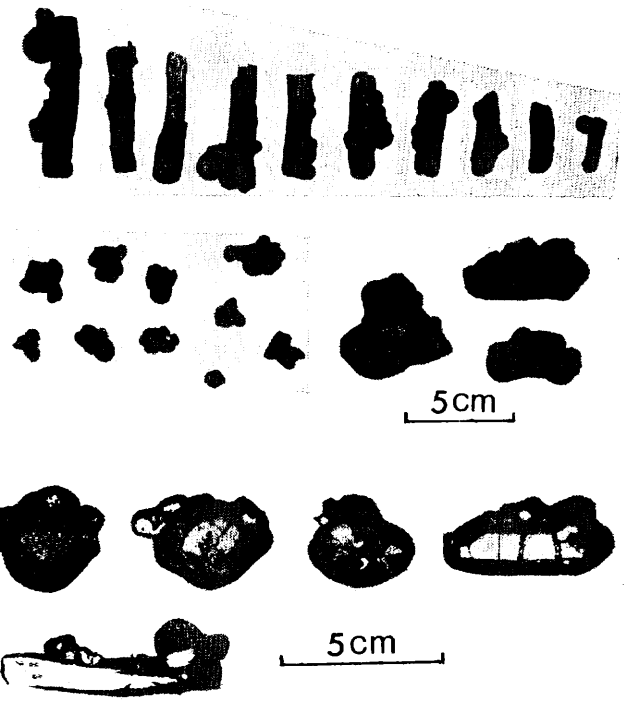

(33)

ST 1073 FG109-1

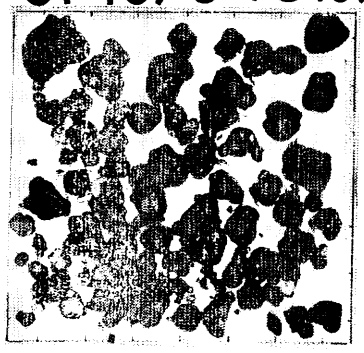

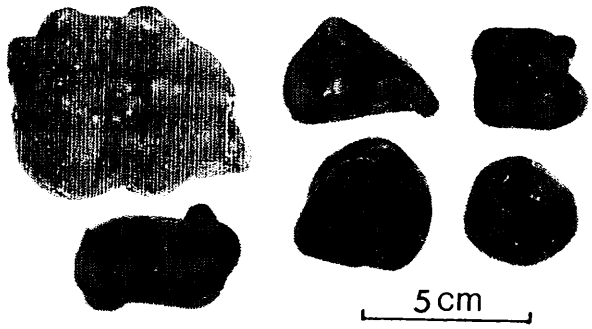

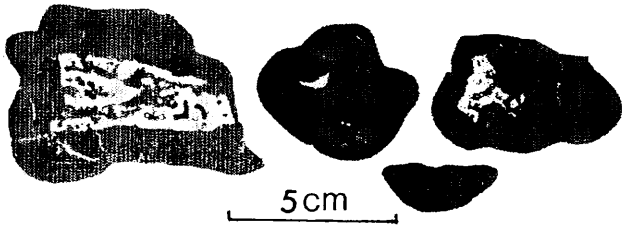

FG109-2

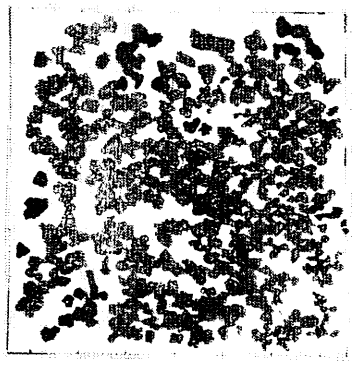

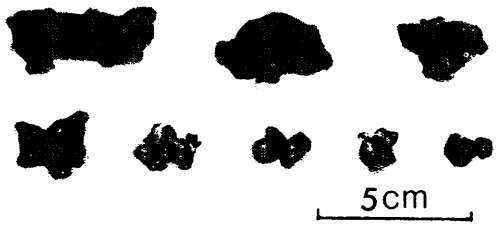

FG109-4

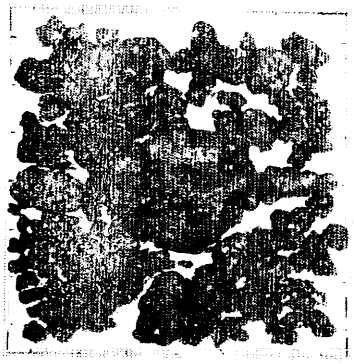

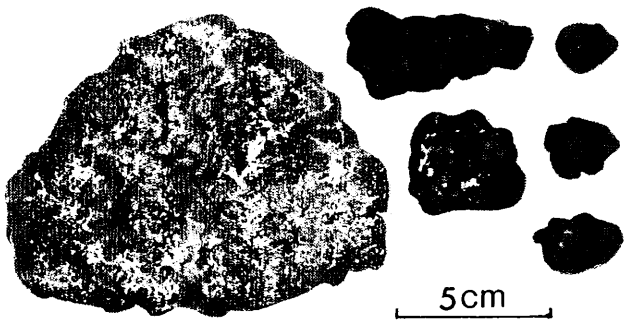

(34)

ST 1072 D262

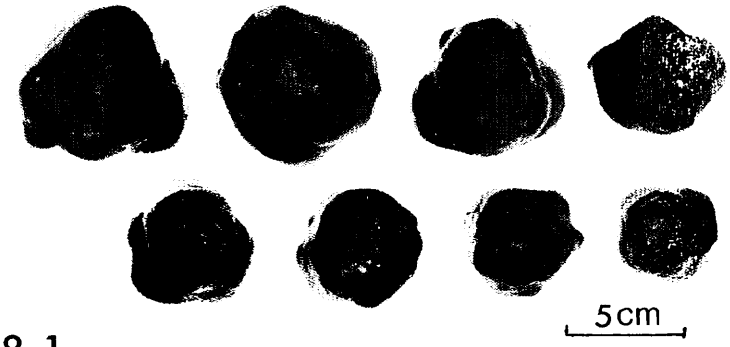

FG108-1

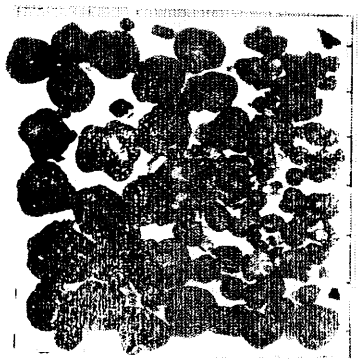

FG108-2

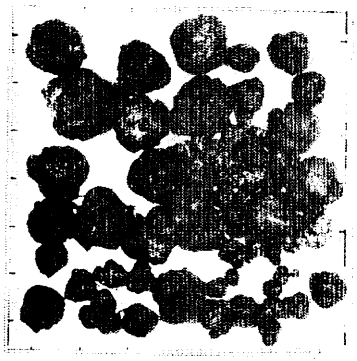

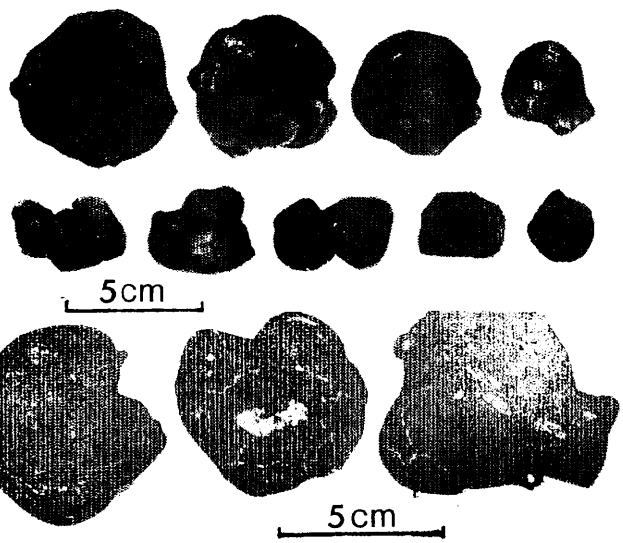

ST 1071 G637

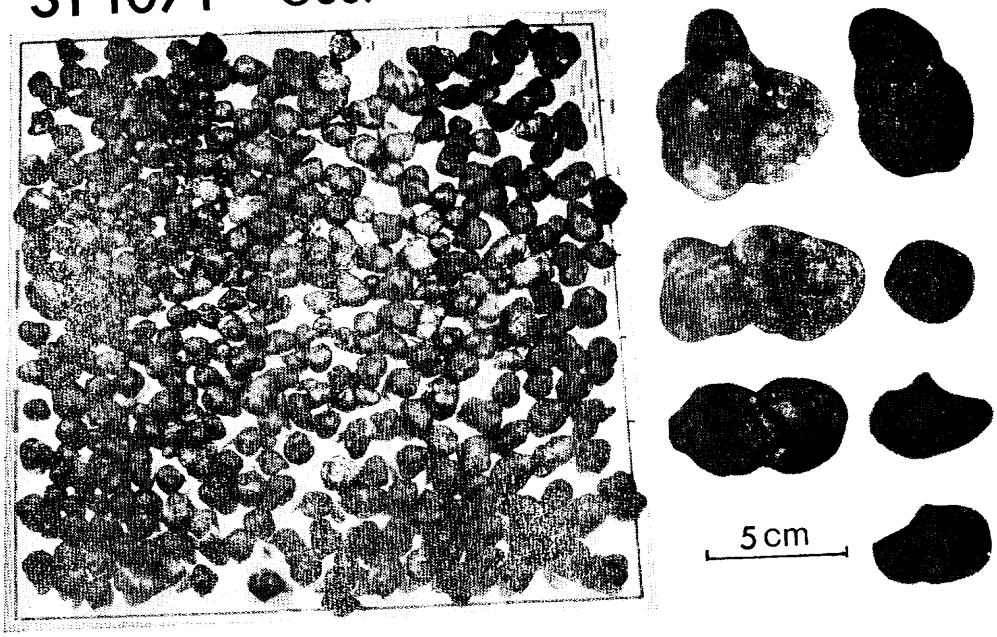

FG107-2

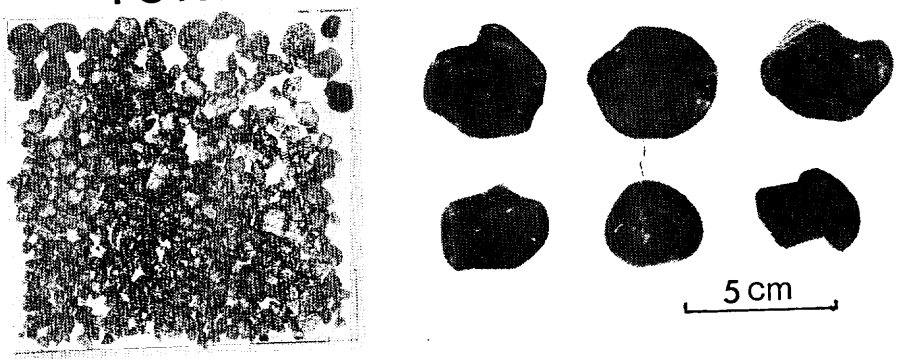

ST 1070 G636

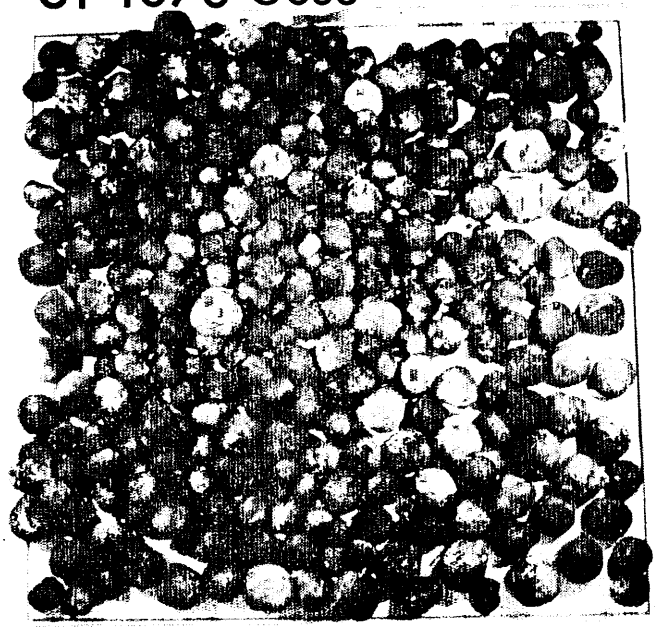

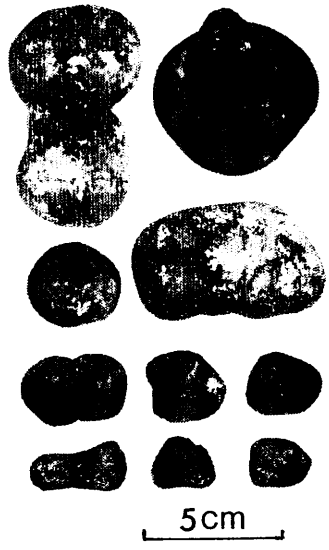

FG106-1

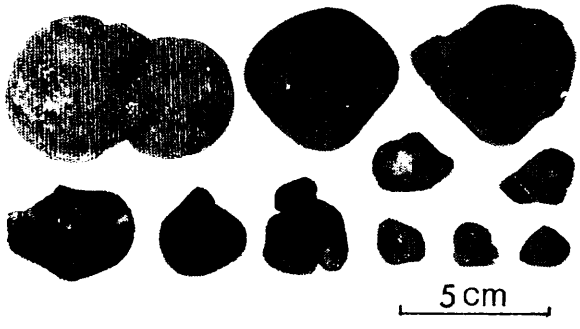

FG106-2

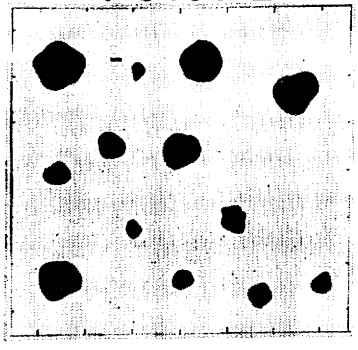

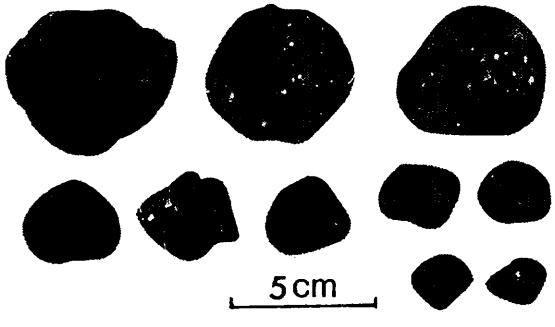

ST 1068 FG104-2

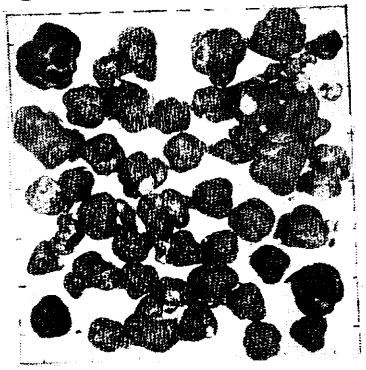

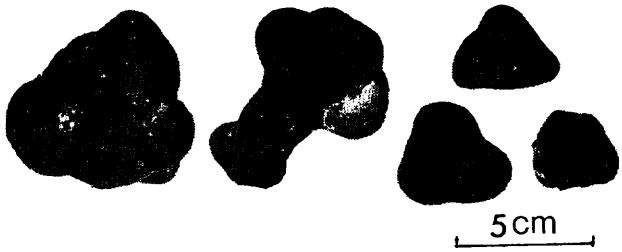

ST 1069 FG105-1

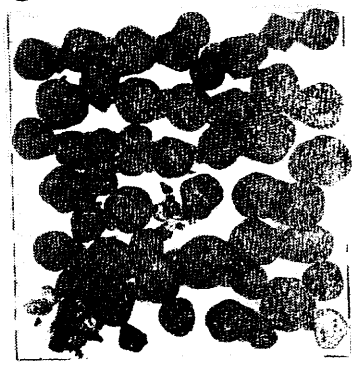

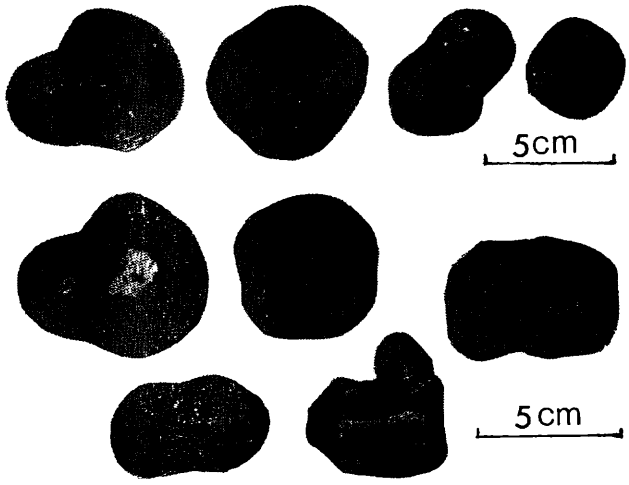

FG105-2

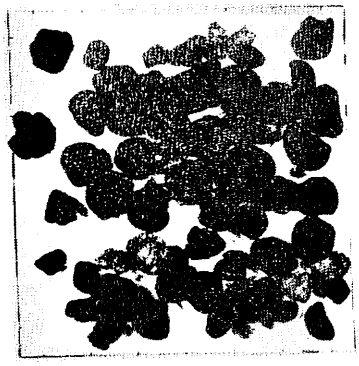

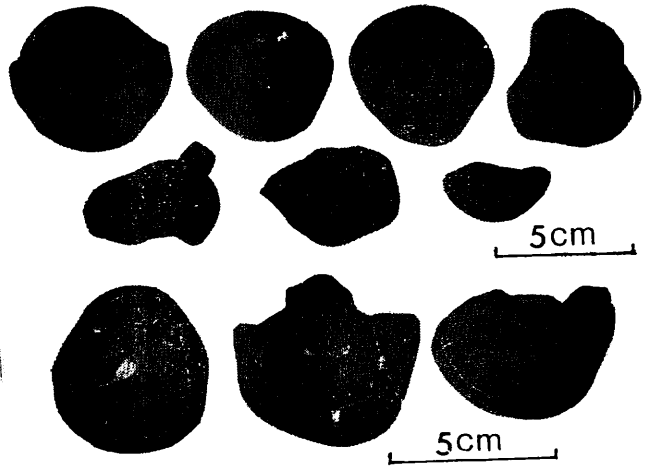

(38)

ST 1067 FG103-1

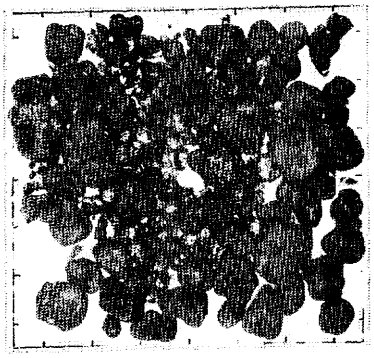

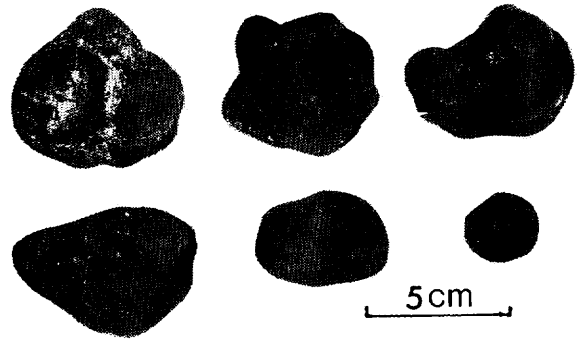

FG103-2

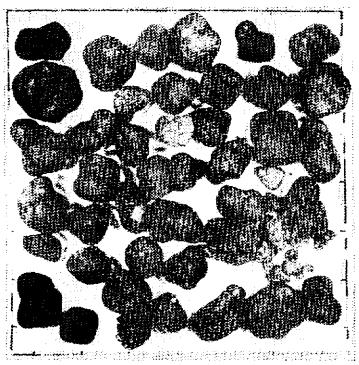

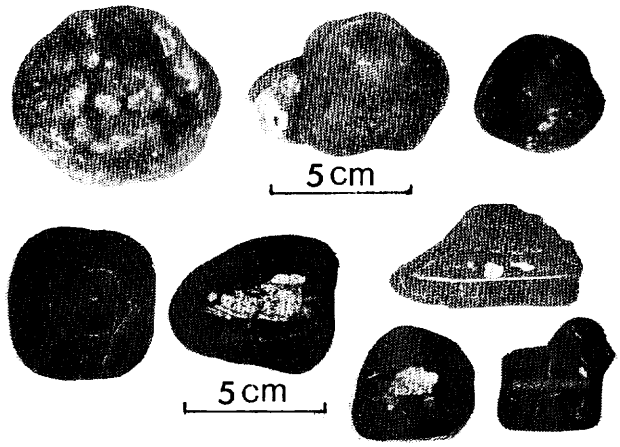

ST 1068 FG104-1

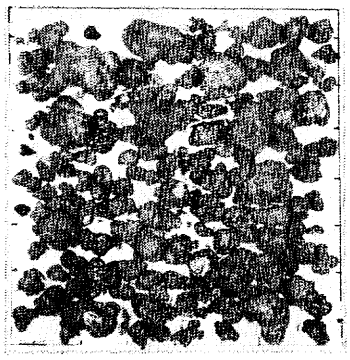

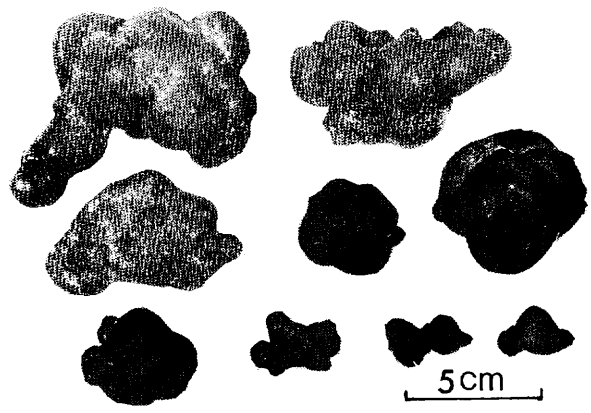

(39)

ST 1067 G634

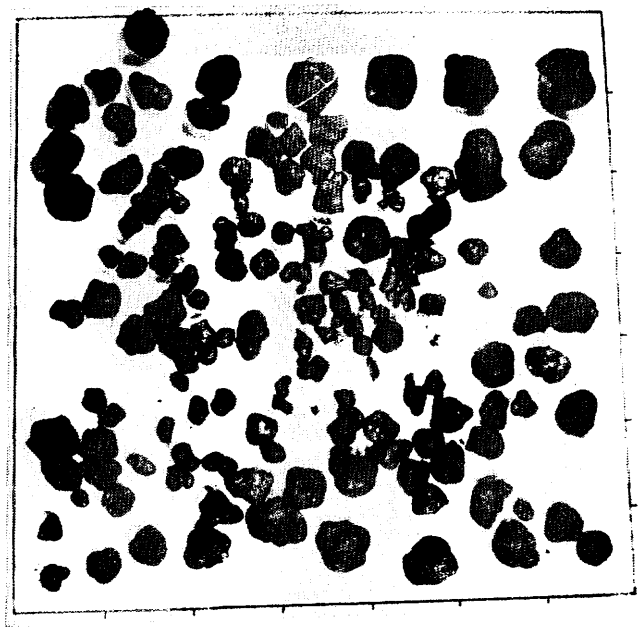

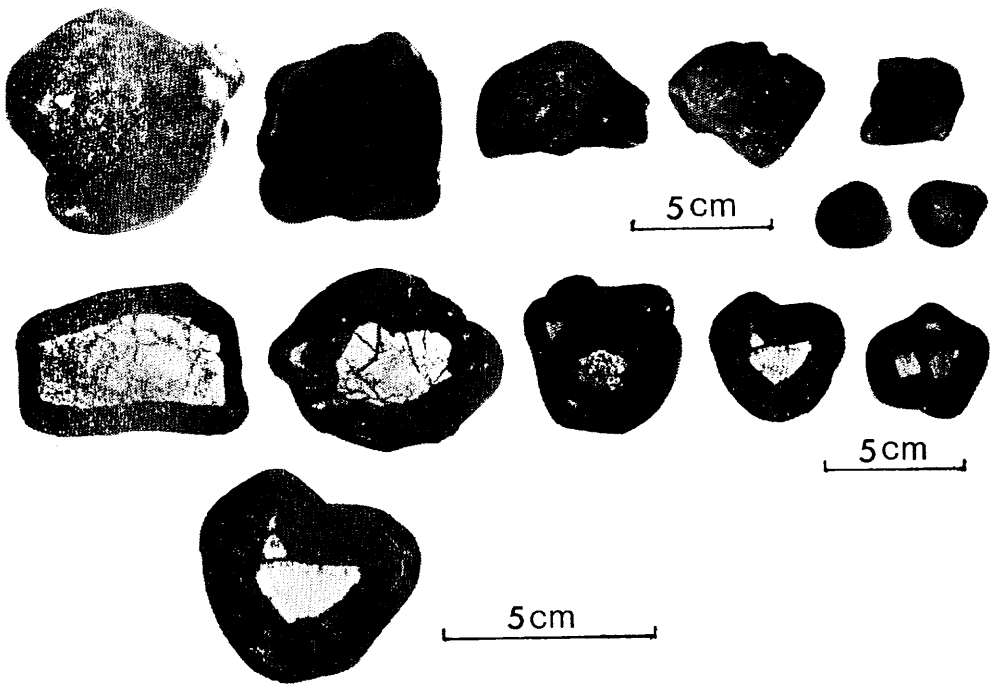

(40)

ST 1065 G632

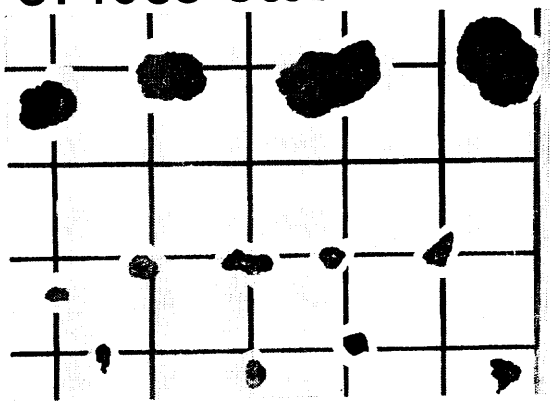

ST1065 FG101-1,2

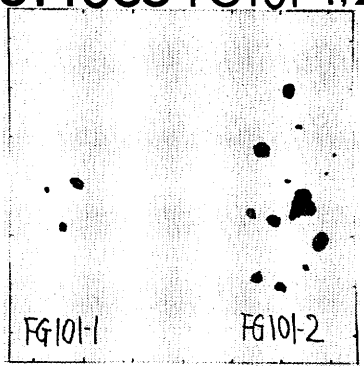

ST 1066 FG102-1

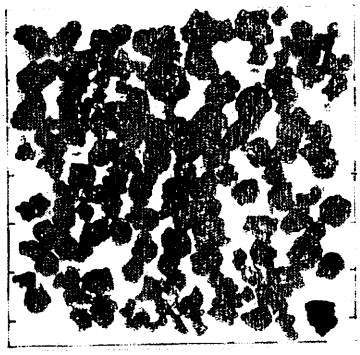

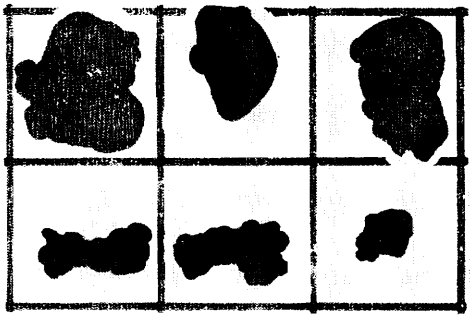

FG102-2

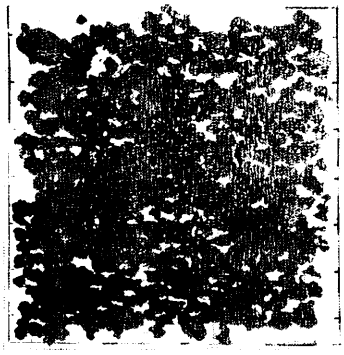

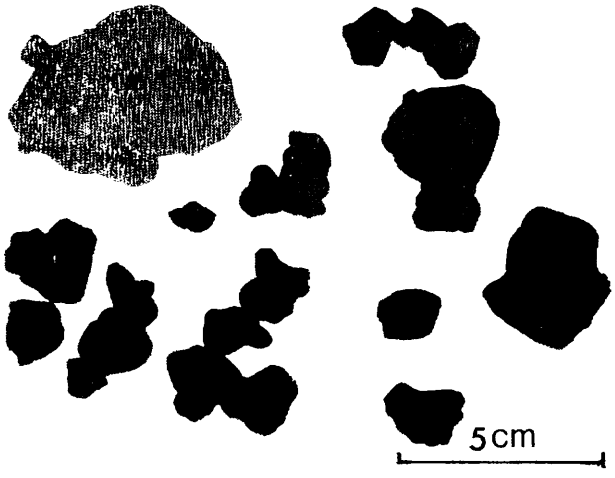

ST 1064 FG100-1

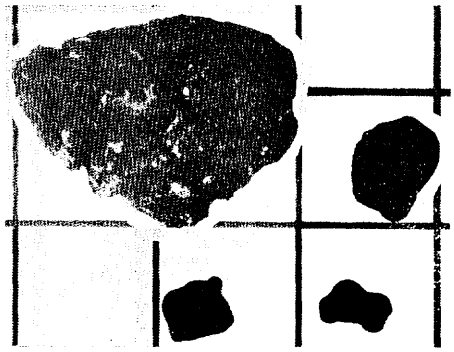

FG100-2

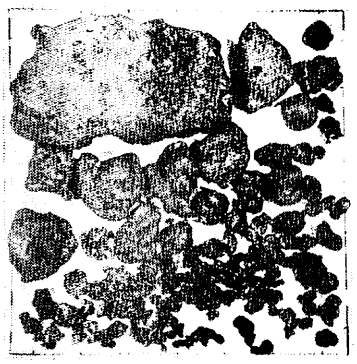

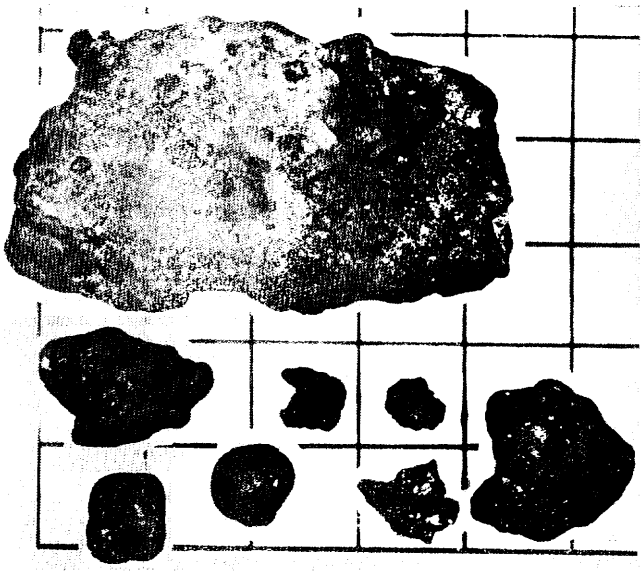

(42)

ST 1061 G(B)624

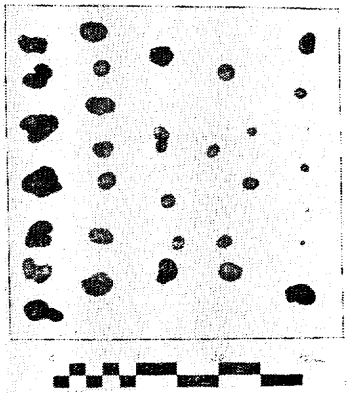

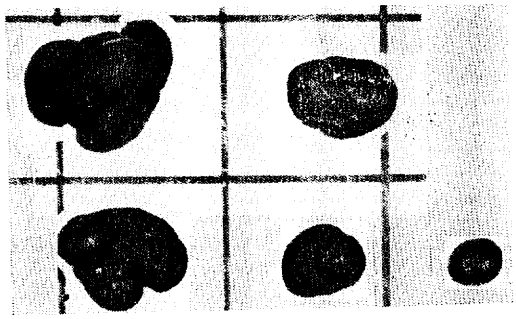

FG93-1

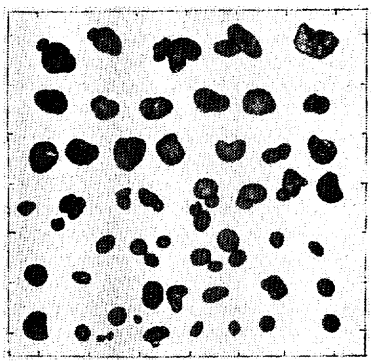

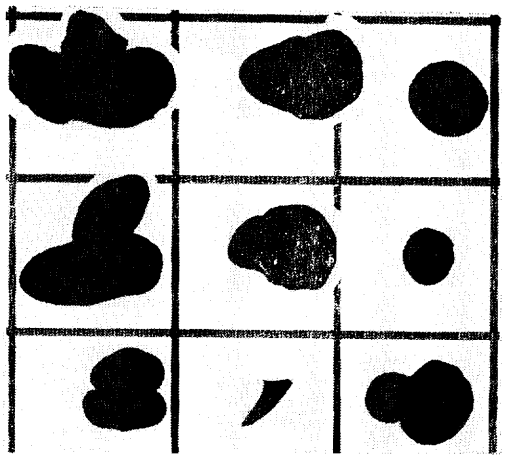

FG93-2

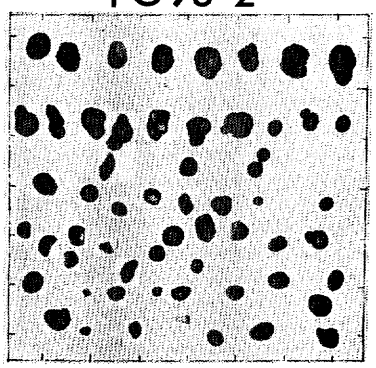

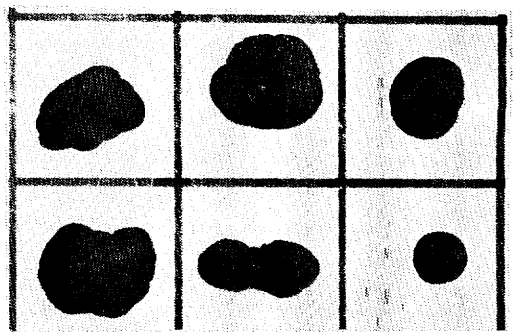

(43)

ST 1060 G(B)623

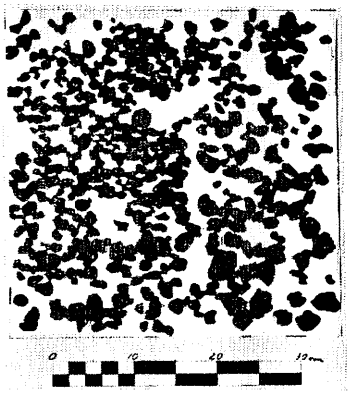

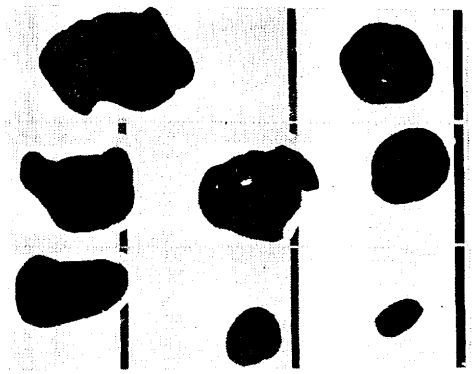

FG 92-1

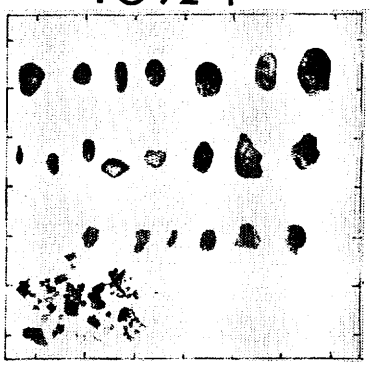

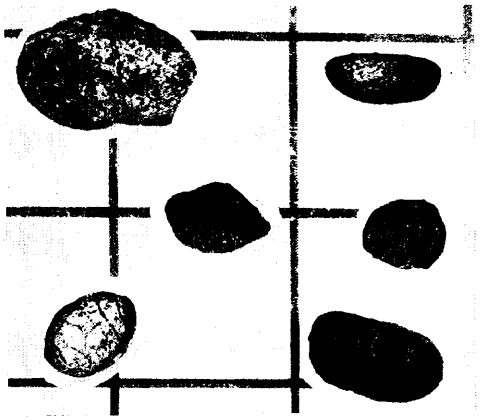

FG92-2

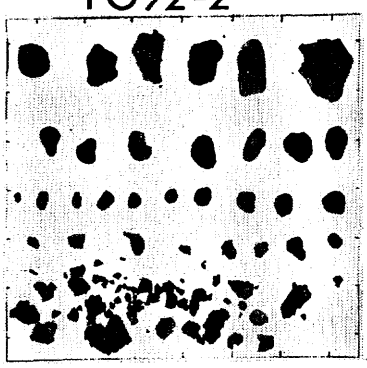

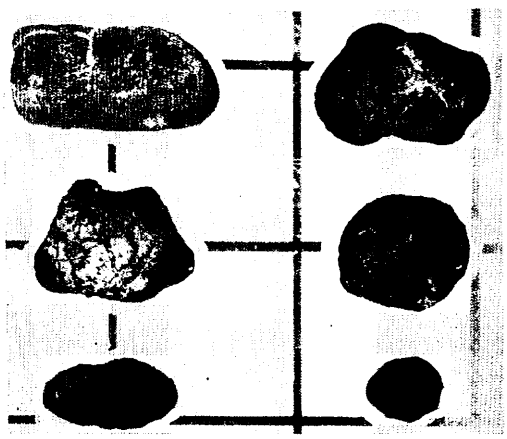

Description of obtained and observed rocks

Rock samples were obtained at the bottom sampling by Okean–70 grab, double spade box corer and freefall grab samplers. Also, existence of rocks was recognized at observation of sea bottom by deep sea camera.

Stations and obtained rock samples are as follows: St. 1039, upper slope of a hill, brecciated basalt; St. 1053, base of a hill, a large number of basalt fragments; St. 1069, slope base of hill, basalt fragment; St. 1040, irregular surface of top of a small hill, chert fragments. Also some exist as relatively large size nuclei of manganese nodules: St. 1045, slope base of a hill, basalt; St. 1048, upper slope of a hill, basalt, St. 1051, irregular surface of top of a hill, consolidated sediments; St. 1073, slope of a hill, phosphorite.

Besides, observation of sea bottom by deep sea camera revealed occurrence of rock fragments at Sts. 1039 and 1059, and outcrop of rock bed at St. 1071.

References

MORITANI, T., MARUYAMA, S., NOHARA, M., KINOSHITA, Y., OGITSU, T. and MORIWAKI, H. (1977) Description, classification, and distribution of manganese nodules. *In* MIZUNO, A. and MORITANI, T. (*eds.*), *Geol. Surv. Japan Cruise Rept.*, no. 8, p. 136–158.

————, ————, ————, ————, KOIZUMI, T. and ITO, T. (1979) Description, types, and distribution of manganese nodules. *In* MORITANI, T. (*ed.*), *Geol. Surv. Japan Cruise Rept.*, no. 12, p. 163–205.